T-1474

AN INVESTIGATION OF THE STRESS CONCENTRATION FACTORS FOR USE WITH THE DOORSTOPPER GAGE

BY

Gary Boyer

T-1474

A Thesis submitted to the Faculty and the Board of Trustees of the Colorado School of Mines in partial fulfillment of the requirements for the degree of Master of Science (Mining Engineering).

Signed: Gary Boyer
Student

Golden, Colorado

Date: May 1, 1972

Approved: W. Hustrulid
Thesis Advisor

Head of Department

Golden, Colorado

Date: May 1, 1972

ABSTRACT

A study has been made of the stress concentration factors needed to obtain field stresses from doorstopper measurements. Based on the results from an experimental program and a finite element study a set of equations for the stress concentration factors which are a function of Poisson's ratio are proposed. Accuracy of the experimental work was confirmed by the use of the United States Bureau of Mines borehole deformation gage in the same borehole as the doorstopper gage.

The proposed functions for the stress concentration factors are:

$$a = 1.2e^{.385\nu}$$

$$b = 0$$

$$c = -0.48-1.2\nu$$

where ν is Poisson's ratio. The functions obtained from the finite element study were partially modified to fit the experimental data, resulting in the equations above.

TABLE OF CONTENTS

LIST OF FIGURES

LIST OF TABLES

ACKNOWLEDGMENTS

The author is deeply grateful for contributions to the success of this investigation made by the following people:

Professors W. Hustrulid, N. Grosvenor, and J. Reed for their advice and suggestions.

The staff of the United States Bureau of Mines Denver Research Center, with special thanks to Messrs. Wilbur Duvall, Vern Hooker, David Bickel and Wilson Blake for the use of their valuable time, equipment and computer facilities.

Fellow students Hans Edlund, and Anil Mayhera for their continual help and encouragement.

The National Science Foundation for providing funds for graduate study.

1. INTRODUCTION

Over the past several years the interest in in-situ stress measurements in rock and the demand for more reliable data have experienced a remarkable growth. Many new techniques and measuring devices have been developed as a result of the intensive research in this field. Of the many instruments developed for stress determinations, only a few are in widespread use. The others, owing to inherent drawbacks in accuracy, ease of operation, or possibly unfamiliarity are used by only a few.

In South Africa the so-called doorstopper gage developed by the Council for Scientific and Industrial Research (CSIR) has become a widely accepted device for stress determinations. With the CSIR doorstopper, a BX borehole is drilled to the point where stress measurements are desired. The core is broken off and the end of the hole is ground smooth with a flat faced diamond bit. The doorstopper, an electrical resistance strain gage rosette mounted in a plastic holder, is cemented to the flattened end of the borehole. After an initial reading, the gage is overcored with the same BX bit used to drill the hole initially. This relieves the stress on the end of the borehole and the doorstopper measures the induced strains. Knowing the elastic constants of the rock, one may then calculate the secondary principal stresses on the borehole end.

The relationship between the measured secondary principal

stresses on the borehole end and the actual principal stresses in the surrounding rock mass is a problem of much concern. The object of this research has been to investigate this relationship.

The doorstopper gage is of interest due to its inherent simplicity, low cost and ease of use. The device can be constructed, inexpensively, by nearly anyone, and its use is not complicated by the need for a large diameter overcore and sophisticated equipment for coring over an electrical cable.

Since the United States Bureau of Mines (USBM) borehole deformation gage has won wide acceptance throughout this country, it was decided to use this device as a standard against which doorstopper readings could be compared. The USBM gage is designed for use in a 1-1/2 inch diameter hole. Thus it was necessary to design and build doorstopper gages for this hole size. To carry out the test work, a polyaxial testing machine was constructed, which allowed both the doorstopper and borehole deformation gages to be used in the same hole. Details of design, construction and testing of the doorstoppers and testing machine are described in appendices to this work.

2. LITERATURE REVIEW

2.1 Introduction

Since many systems of stress notation are in use in the rock mechanics field, it will be helpful to define the system that is used throughout this thesis. The many authors cited have used different notations. These diverse systems have been converted to a common system for use in this thesis, making equations and symbols appear somewhat different than in the original work.

Field stresses, or virgin stresses, in the rock surrounding a borehole will be donated by:

S_1 in the plane of the borehole end

S_2 in the plane of the borehole end

S_3 parallel to the borehole

These are the normal components of the principal stresses acting in the rock mass and are the stresses of interest in in-situ measurements. Shear stresses are usually of little interest in this type of work and will not be dealt with here. Tension is considered to be positive and conversely compression is negative.

Secondary principal stresses on the borehole end will be donated by:

σ_{max} the radial stress of greatest magnitude

σ_{min} the radial stress of least magnitude

(regardless of sign)

The stress concentration factors (SCF) for the borehole end

as originally defined by Leeman (1) will be used:

SCF a The contribution, to the stress concentration on the borehole end, from the principal field stress in the plane of and parallel to the measured stress.

SCF b The contribution, to the stress concentration on the borehole end, from the principal field stress in the plane of and perpendicular to the measured stress.

SCF c The contribution, to the stress concentration on the borehole end, from the principal field stress parallel to the axis of the borehole.

Thus as a general condition we may write:

$$\sigma_{max} = aS_1 + bS_2 + cS_3 \qquad (2.1)$$

$$\sigma_{min} = aS_2 + bs_1 + cS_3 \qquad (2.2)$$

A mathematical solution for the determination of constants a, b & c does not exist. Determinations have been made experimentally and by the method of finite element analysis. There is wide disagreement throughout the literature for the value of these constants.

2.2 Determination of SCF a and b

The first work done by Leeman (1) was to place cubes of granite, steel and araldite, fitted with doorstopper gages, in uniaxial compression in a testing machine. The measured stress

on the borehole end in the direction of the applied stress was near 1.53 times the applied stress for all three specimens. The magnitude of the measured stress perpendicular to the applied stress was less than 8% of that measured parallel to the applied stress. Leeman concluded that this was due to frictional effects from the machine platens, and that in a purely uniaxial field the stress perpendicular to the applied stress would be zero. Thus he determined that constant $a = 1.53$ and constant $b = 0$.

Galle (2) and later Galle and Wilhoit (3) made three dimensional photoelastic studies of the stresses on a borehole end, prior to Leeman's work, using epoxy resin models. They also reported that $a = 1.53$ and later 1.56 and that $b = 0$. In addition, Galle plotted the variation of stress along the diameter of the borehole end and found that it was uniform for about 0.4 times the radius from the center. See fig. 2.1.

Hoskins (4), using trachyte cubes in biaxial compression, determined that $a = 1.56$ and $b = 0$.

Bonnechere (5), using 6 inch plexiglass cubes in uniaxial compression, determined values of $a = 1.56$ and $b = 0$.

Bonnechere and Fairhurst (6), also using 6 inch plexiglass cubes in uniaxial compression, determined that $a = 1.26$ for the cube tested between steel platens, and $a = 1.23$ for the cube tested between two other plexiglass cubes. For both conditions, they found the stress perpendicular to the applied stress to be

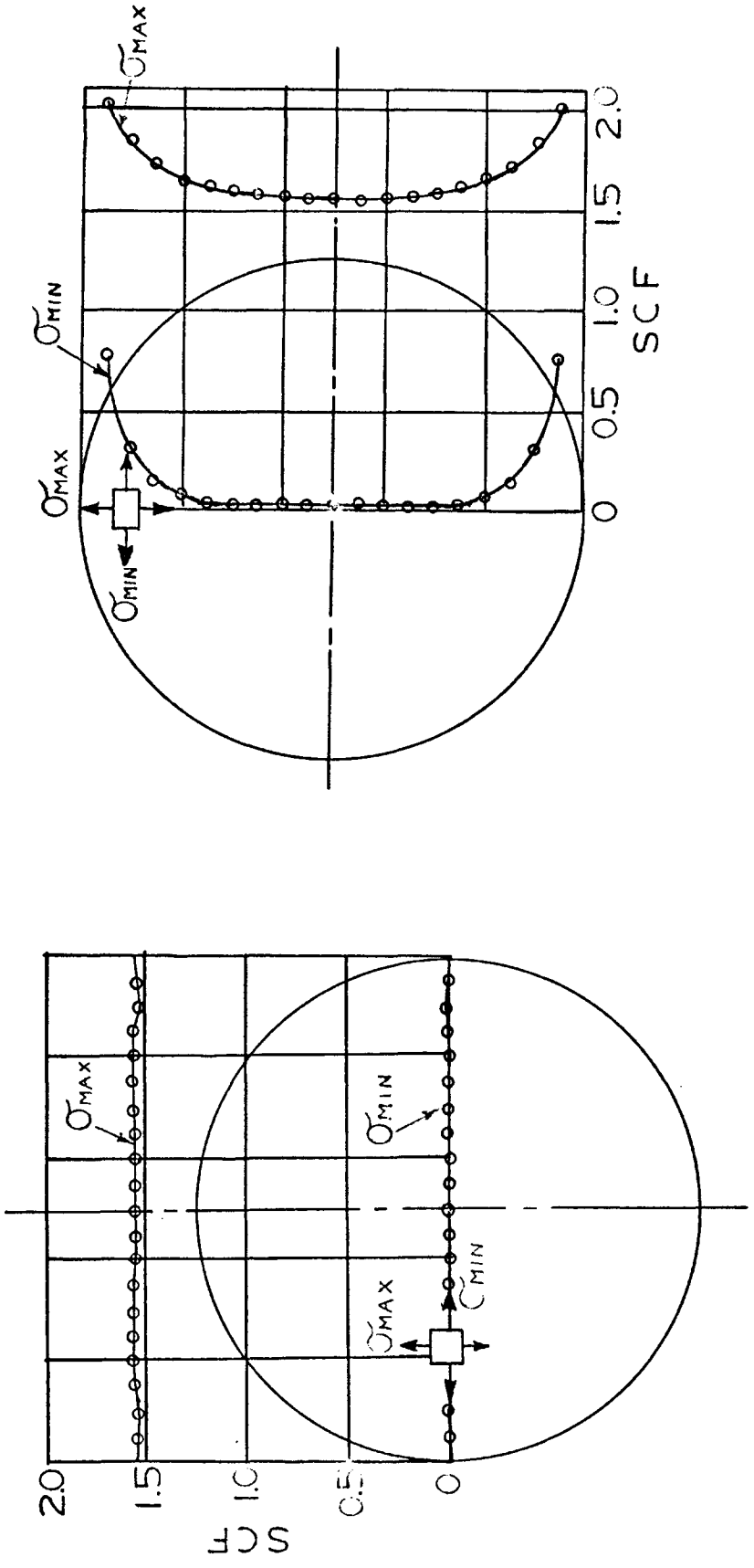

fig. 2.1 Stress concentrations along the horizontal and vertical diameters of the flat end of a borehole subjected to a uniaxial vertical stress S_1.
(Galle and Wilhoit)

negligable and thus $b = 0$. They also studied the effect of a shear stress acting parallel to the axis of the borehole by loading plexiglass cubes with inclined boreholes, that is boreholes not parallel or perpendicular to the applied stress. The results showed the effect of the shear stress to be negligable, supporting what would be predicted by elastic theory. This confirms the assumption that shear stresses need not be considered in stress measurements made by doorstoppers.

Pallister, (7), using steel and aluminum cylinders loaded biaxially by means of quadranted jacks, reported values of $a = 1.1$ and $b = 0$.

Van Heerden (8) postulated that it was not possible to obtain uniform stress fields in cubes and made a series of tests using blocks and cylinders with a 2:1 height to width ratio. He first investigated the situation photoelastically using epoxy resin models. The models were loaded uniaxially in the direction of the longer dimension. The stresses were frozen in and the model sliced into thin wafers for analysis in the polariscope. By taking slices in the proper direction, he was able to analyze the stress concentration factors a and b independently. From this study he concluded that $a = 1.25$ and $b = -.071$. Next he conducted uniaxial compression tests on an aluminum cylinder and on blocks of steel, sandstone and norite. The boreholes were placed at the mid-height of the specimens and fitted with strain gage rosettes

on the borehole ends. Van Heerden measured values of SCF a ranging from 1.22 for norite to 1.31 for sandstone. He measured values of SCF b ranging from -0.022 for aluminum to -0.19 for sandstone. A complete tabulation of his results will be found in table 2.5. Van Heerden also confirmed the earlier work by Galle, showing that the stress distribution is uniform across the center 0.4 of the borehole end. See fig. 2.2.

Hiramatsu and Oka (9) using photoelasticity were perhaps the first to establish a definite relationship between the stress concentration factors a and b and Poisson's ratio. They showed that there is a definite trend of increase in a and b with an increase in Poisson's ratio. They investigated materials with a range of Poisson's ratio from 0.24 to 0.44 and determined SCF a from 1.36 to 1.42 respectively. For the same spread in Poisson's ratio they determined SCF b to range from -0.304 to -0.060. See table 2.5. This work resulted in several other researchers investigating the effect of Poisson's ratio.

Crouch (10) using the finite element technique, assumed that SCF b was equal to zero and set up an axisymmetric program for the determination of SCF a for values of Poisson's ratio from 0 to 0.4. The results of this work indicate very little dependence on Poisson's ratio, the values of SCF a grouping very close to 1.23. See fig. 2.3.

In another finite element study, Coates and Yu (11) used both

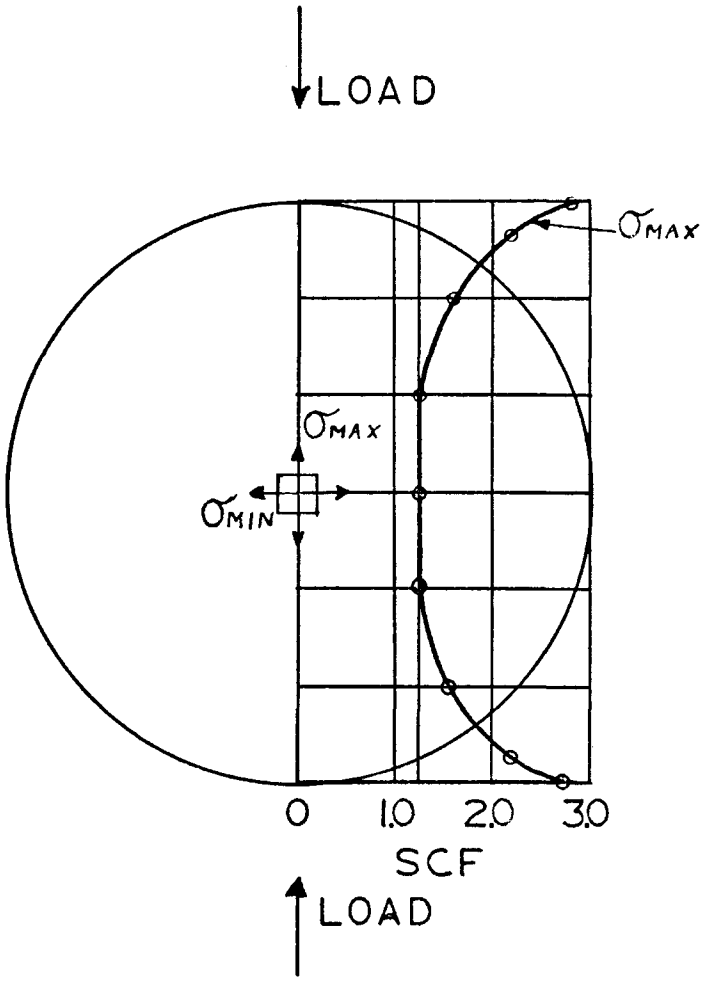

fig. 2.2 Stress concentration along the vertical diameter of a flat ended borehole. (Van Heerden)

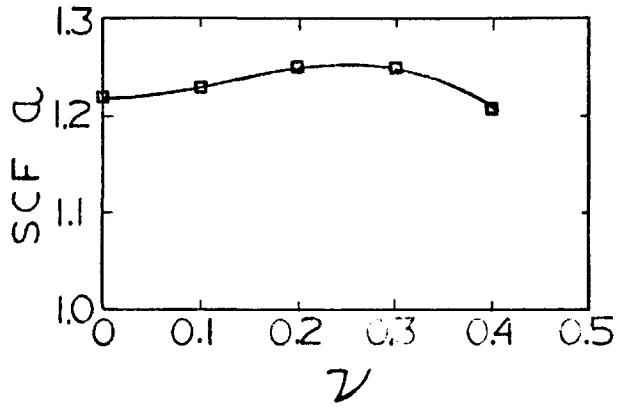

ν	a
0	1.22
0.1	1.23
0.2	1.25
0.3	1.25
0.4	1.21

fig. 2.3 Stress concentration factor a as a function of Poisson's ratio. (Crouch)

axisymmetric and non-axisymmetric programs to obtain the stress concentration factors a and b independently and in combination. With the axisymmetric program only the sum of a and b could be determined since an equal pressure is applied in all directions around the borehole. However, with the non-axisymmetric programs, uniaxial radial boundary pressures could be applied and SCF a and b could be determined independently. Comparison of results between the two types of programs is excellent. The results indicate values of SCF a which fall about midway between the early measurements by Leeman and Galle and later measurements by Bonnechere and Van Heerden. Coates and Yu also determine, as did Hiramatsu and Oka, that SCF b has small finite values which are a function of Poisson's ratio. However, the values of the former are much different than that of the latter. By regression analysis, Coates and Yu determine the following functions:

$$a = 1.366 + 0.025\nu + 0.502\nu^2 \qquad (2.3)$$

$$b = -0.125 + 0.154\nu + 0.390\nu^2 \qquad (2.4)$$

where ν is Poisson's ratio. See figs. 2.4 and 2.5. A tabulation of their results will be found in table 2.1. Coates and Yu also plotted the variation of the radial stress across the diameter of the borehole end. See fig. 2.6.

2.3 Determination of SCF c

Early researchers recognized that SCF c would be sensitive

to Poisson's ratio since the axial stress on the borehole is applied perpendicular to the surface on which strains are measured. However, little work was done in determining a function for c as it was assumed that its effect would be negligable if S_3 was the least principal stress. For this reason it has been common practice to assume the direction of S_3 and orient the borehole in this direction.

Leeman (1) decided from some early tests that if S_3 was small compared to S_1, the error introduced by neglecting it would be small. As an example, he stated that if $S_3 = 1/3\ S_1$, the error in computing S_1 will be on the order of 5% for rocks having a Poisson's ratio of 0.15.

Galle and Wilhoit (3) using photoelasticity and later Hoskins (4) testing trachyte cubes in biaxial compression both reported a value of $c = -1.04$. The epoxy resin models used by Galle and Wilhoit had a Poisson's ratio of 0.47. Hoskins' trachyte had a Poisson's ratio of 0.22.

Extending the work of Bonnechere (5), Bonnechere and Fairhurst (6) found a value of $c = -0.685$ for the plexiglass cube tested between two steel platens and $c = -0.661$ for the cube tested between two other plexiglass cubes. They decided on a mean value of $c = -0.67$ for a plexiglass with Poisson's ratio of 0.38. Thus they suggested a function:

$$c = -0.75\ (0.5+\nu) \qquad (2.5)$$

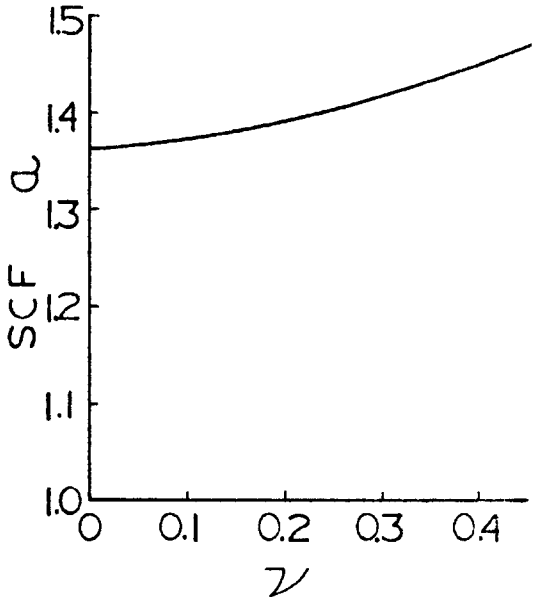

fig. 2.4 Variation of SCF a with Poisson's ratio. (Coates and Yu)

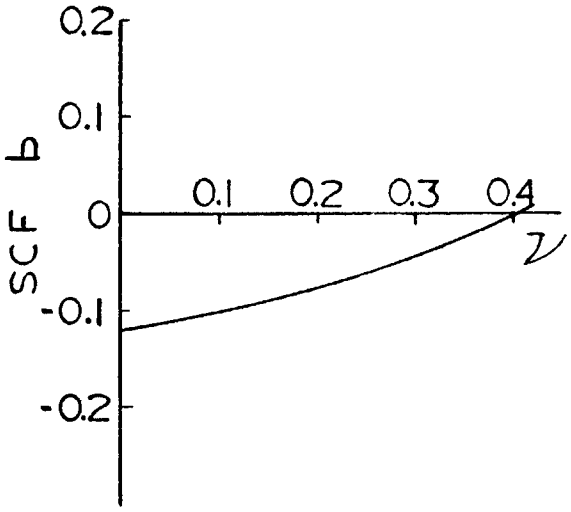

fig. 2.5 Variation of SCF b with Poisson's ratio. (Coates and Yu)

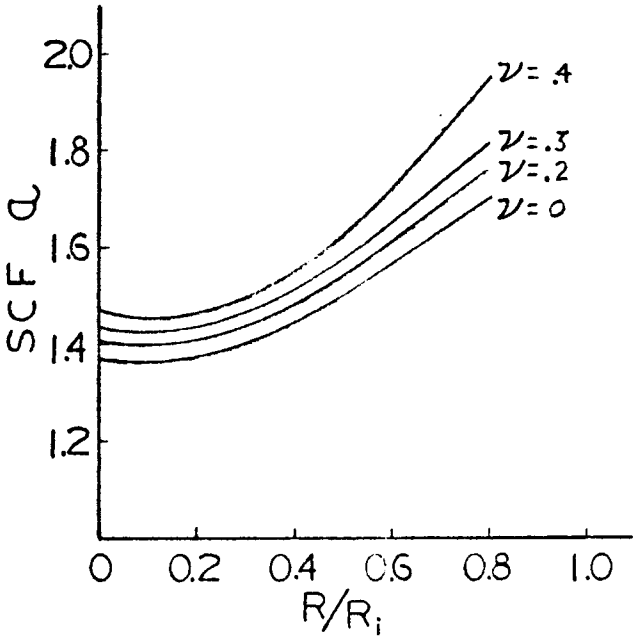

fig. 2.6 Variation of SCF a as distance from borehole axis (R) along the borehole radius (R_i). (Coates and Yu)

TABLE 2.1

Stress Conditions	ν	a	b	a + b	program type
$S_2 = S_3 = 0$	0.0	1.36	-0.12	1.24	non-axisymmetric
$S_1 = 1$	0.2	1.40	-0.08	1.32	
	0.3	1.41	-0.04	1.36	
	0.4	1.45	0.0	1.45	
$S_1 = S_2 = 1$	0.0			1.24	axisymmetric
$S_3 = 0$	0.2			1.32	
	0.3			1.38	
	0.4			1.47	

Stress concentration factors a and b as determined by Coates and Yu.

Pallister (7) using steel and aluminum cylinders loaded biaxially reported a value of $c = -0.75$ for a Poisson's ratio of 0.29.

Van Heerden (8) in his study using blocks with a 2:1 height to width ratio measured 3 different values of c at 3 different values of Poisson's ratio. Using blocks of aluminum, steel and norite, he measured values of $c = -0.74, -0.72, -0.69$ respectively. These values correspond to Poisson's ratios of $\nu = 0.352, 0.308, 0.273$. From these data he suggested the relationship:

$$c = -0.75\ (0.645 + \nu) \qquad (2.6)$$

which is reasonably close to that suggested by Bonnechere and Fairhurst. See fig. 2.7.

The photoelastic studies by Hiramatsu and Oka (9) show a greater increase in c with increasing Poisson's ratio than do the studies by Van Heerden. Hiramatsu and Oka studied materials with a Poisson's ratio range of 0.24 to 0.44 and measured corresponding values of c from -0.69 to -1.10. This compares favorably with Van Heerden's values at the lower values of ν but is much different at the higher values. Compare the complete listing in table 2.5.

Crouch (10) has determined values of c with his axisymmetric finite element analysis for $\nu = 0, 0.1, 0.2, 0.3$ and 0.4. These values of c compare very favorably with the relationship proposed by Van Heerden in equation (2.5) above. See table 2.2.

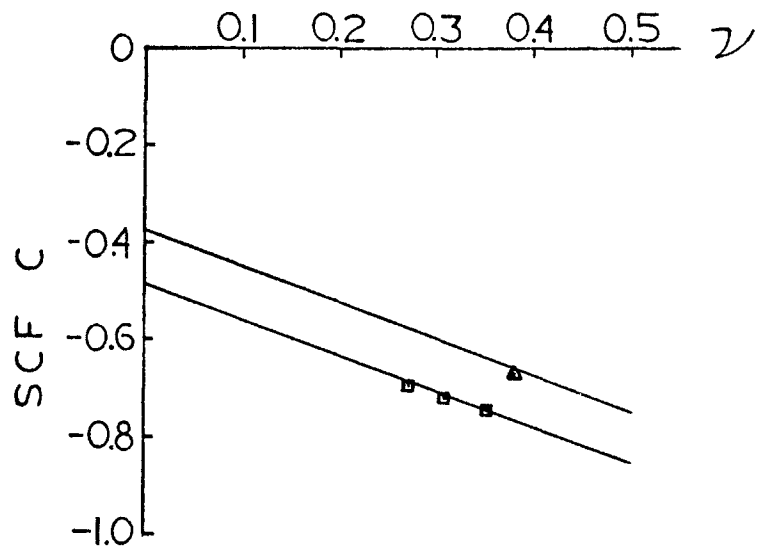

fig. 2.7 Comparison of functions for SCF c as determined by Bonnechere (△) and Van Heerden (□).

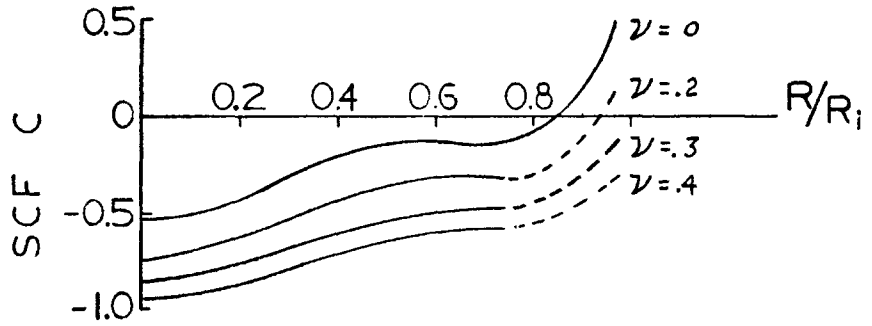

fig. 2.8 Variation of SCF c as distance from borehole axis (R) along the borehole radius (R_i). (Coates and Yu)

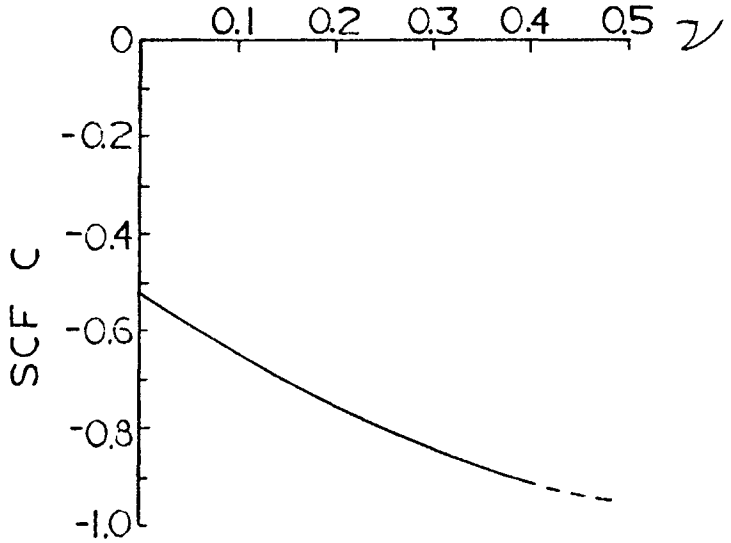

fig. 2.9 Stress concentration factor c as a function of Poisson's ratio. (Coates and Yu)

TABLE 2.2

	Crouch	Van Heerden
ν	c	$c = -0.75(0.65 + \nu)$
0	-0.455	-0.48
0.1	-0.540	-0.56
0.2	-0.620	-0.63
0.3	-0.700	-0.71
0.4	-0.780	-0.78

Comparison of c values as determined by Crouch and Van Heerden

The finite element study by Coates and Yu (11) shows a trend in c similiar to those proposed by Van Heerden and Hiramatsu and Oka. However, there is no real agreement in the exact values. Coates and Yu determined values of c with both axisymmetric and non-axisymmetric programs and again, as with factors a and b got excellent comparisons. A regression analysis of the data suggests the relationship:

$$c = -0.520 - 1.331\nu + 0.886\nu^2 \qquad (2.7)$$

The specific values are tabulated in table 2.3.

There is one interesting mathematical analysis which may be compared to the stress concentrations at the end of a borehole. Terzaghi and Richart (12) have published the analytical solution for a spheroidal (ellipsoid of revolution) cavity under stress parallel to the axis of revolution. The tangential stress in a radial plane, at the surface of spheroid with 50:1 major to minor axis ratio was calculated for different values of Poisson's ratio. The calculated stresses are constant over roughly the center 0.4 of the radius paralleling the photoelastic work on a borehole bottom done by Galle and Van Heerden. The values of the stress concentration factors (comparable to c for a flat ended borehole) are surprisingly close to the values obtained by Coates and Yu. Compare the values in table 2.4.

Comparing the radial stress concentrations on a flat ended borehole to the tangential stress concentrations on the surface

TABLE 2.3

Stress Conditions	ν	c	program type
$S_1 = S_2 = 0$	0.0	-0.52	axisymmetric
$S_3 = 1$	0.2	-0.75	
	0.3	-0.84	
	0.4	-0.91	
$S_1 = S_2 = 0$	0.2	-0.76	non-axisymmetric
$S_3 = 1$			

Stress concentration factor c as determined by Coates and Yu.

TABLE 2.4

ν	Radial stress concentration on flat borehole end (Coates and Yu)	Tangential stress concentration on surface of spheroidal cavity (Terzaghi and Reichart)
0	-0.52	-0.49
0.1	-----	-0.59
0.2	-0.75	-0.70
0.3	-0.84	-0.81
0.4	-0.91	-0.91

of a spheroidal cavity may be a somewhat rough analogy, but the similarity of results is interesting. See fig. 2.10.

2.4 Some Field Measurements

It is the purpose of this section to present some actual field measurements made by several investigators with particular emphasis on those where doorstopper measurements were compared to the USBM borehole deformation gage. The literature contains a number of publications where results of doorstopper and borehole deformation gage measurements are presented. Unfortunately a detailed analysis of how the results were obtained is missing in most of these publications. For this reason the author has chosen a few papers, which contain a detailed analysis, for summary here.

Leeman (13) in some early work used doorstoppers to measure stress in the sidewalls of a hoist chamber 5800 feet underground. Using stress concentration factors of $a = 1.53$, $b = 0$, and assuming the effect of c is negligable (which is a reasonable assumption when measuring stress in an abutment near a free face) he obtained vertical stress values of roughly twice the gravity overburden stress. Leeman concluded that the high value of vertical stress was probably due to stress concentrations caused by the hoist chamber itself. He also measured a vertical:horizontal stress ratio of 2:1 which is close to what would be predicted by elastic theory assuming complete lateral restraint. The use of

TABLE 2.5

Investigator	Poisson's ratio	Stress concentration factor		
		a	b	c
Galle	0.48	1.53	0	---
Galle & Wilhoit	0.47	1.56	0	-1.04
Leeman	0.26	1.53	0	---
	0.29	1.51	0	---
	0.48	1.55	0	---
Hoskins	0.22	1.56	0	-1.04
Pallister	0.29	1.10	0	-0.75
Bonnechere	0.38	1.25	0	---
Bonnechere & Fairhurst	0.38	1.25	0	-0.67
Van Heerden	0.25	1.31	-0.19	---
	0.261	1.22	-0.098	---
	0.273	---	---	-0.69
	0.287	1.24	-0.065	---
	0.308	---	---	-0.72
	0.35	1.28	-0.022	---
	0.352	---	---	-0.74
	0.48	1.25	-0.071	---
Hiramatsu & Oka	0.24	1.36	-0.304	-0.69
	0.29	1.32	-0.289	-0.82
	0.37	1.39	-0.204	-0.98
	0.44	1.42	-0.060	-1.10
Crouch	0	1.22	0	-0.455
	0.1	1.23	0	-0.540
	0.2	1.25	0	-0.620
	0.3	1.25	0	-0.700
	0.4	1.21	0	-0.780
Coates & Yu	0	1.36	-0.12	-0.52
	0.2	1.40	-0.08	-0.75
	0.3	1.41	-0.04	-0.84
	0.4	1.45	0	-0.91

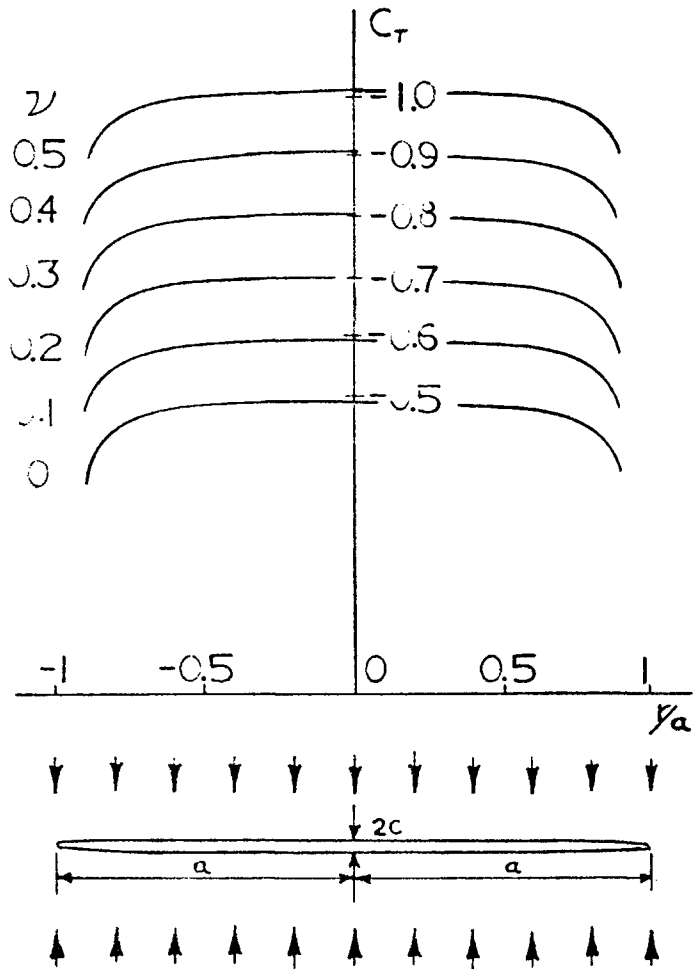

fig. 2.10 Tangential stress concentration factors (C_t) on the surface of a spheroidal cavity with 50:1 major to minor axis (a:c) ratio. (Terzaghi and Richart)

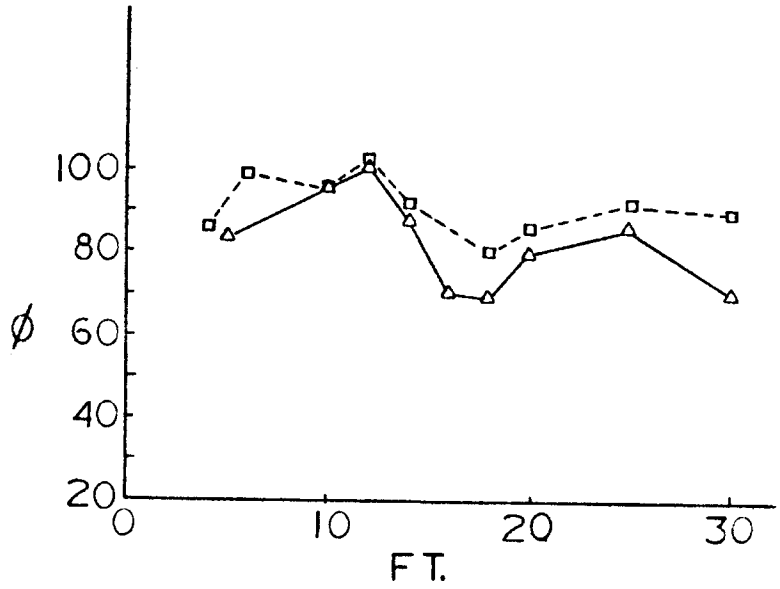

fig. 2.11 Variation of the major principal stress direction ϕ (degrees from vertical) with distance into the solid. (Van Heerden and Grant)
—△—USBM gage
--□-- Doorstopper

a lower value of SCF a would have resulted in an even higher value of the vertical stress. Leeman's conclusion was probably accurate, and he was in fact measuring a stress concentrated by the mine hoist chamber.

Van Heerden and Grant (14) have made an exhaustive comparison of doorstopper vs. USBM borehole deformation gage measurements at a depth of 1400 feet in an abandoned area of a large mine. Measurements were made in two areas: Area 1 was in the wall of an extension drift remote from any other openings and approached virgin rock conditions. Area 2 measurements were made in pillars. In both areas, measurements were taken in boreholes drilled parallel and close to one another. The two gages were necessarily in different boreholes. Stress concentration factors for the borehole end were assumed to be the same as used by Leeman (13) above.

Comparison of results from the two gages was generally very good, on the average. The borehole deformation gage indicated the principal stresses to be consistently higher than those indicated by the doorstoppers. Van Heerden and Grant discussed a number of reasons why this could have happened. It is the author's opinion, however, that the most likely reason for the difference in readings is the use of the stress concentration factor $a = 1.53$. The use of a lower value for a would bring the values of the principal stresses very close to those indicated by the borehole

deformation gage. The use of a stress concentration factor of a = 1.30 would raise the value of the major principal stress by about 18%, bringing the results from the two gages very close together.

Measurements taken from the extension drift were done at 2-5 foot intervals for 30 feet into the sidewall. If one compares the individual determinations of the principal stresses at various depths into the sidewall a curious thing appears. Measurements of the maximum principal stress are fairly consistent for both gages, having a magnitude change on the order of 2:1. Measurements of the minimum principal stress made by the doorstopper, however, are extremely inconsistent, having a magnitude change of as much as 30:1. See table 2.6. This indicates that any one measurement made by the doorstopper can give a reasonable estimate of the vertical stress, but the indication of horizontal stress may be absolutely meaningless. The author has no explanation for this situation, but experienced the same problem in his own work. See figs. 2.11, 2.12 and 2.13.

Stephenson and Murray (15) have made a comparative study of doorstopper vs. flat jack stress measurements under field conditions at a depth of 1200 feet. The field tests were quite complete, taking measurements at different locations throughout the 1200 foot level of the mine. Measurements were taken in three orthogonal directions so that the complete stress tensor could be

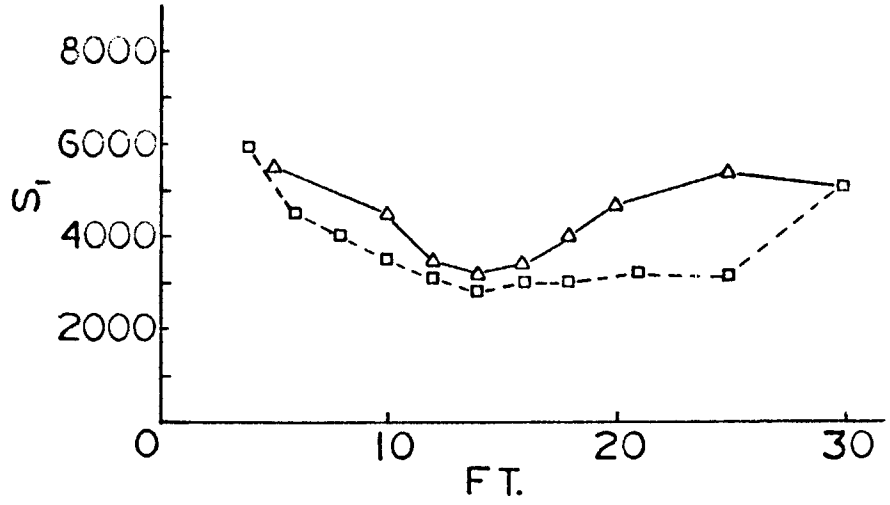

fig. 2.12 Variation of the major principal stress (psi) with distance into the solid. (Van Heerden and Grant)
—△—USBM gage
--□-- Doorstopper

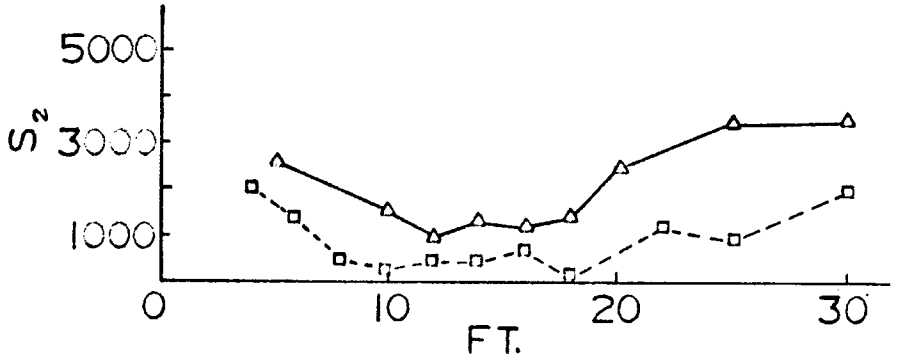

fig 2.13 Variation of the minor principal stress (psi) with distance into the solid. (Van Heerden and Grant)
—△—USBM gage
--□-- Doorstopper

TABLE 2.6

Depth of hole (ft.)	Principal stresses (psi) S_1	S_2	Angle (degrees from vertical) ϕ
U.S.B.M. Deformation Meter results - Borehole No. 1			
5	5542	2580	84
10	4469	1573	95
12	3497	940	101
14	3220	1307	88
16	3457	1209	70
18	4017	1427	69
20	4806	2448	80
25	5514	3543	86
30	5060	3540	70
C.S.I.R. Strain Gage Strain Cell Borehole No. 2			
4	4700	1000	82
6	3300	340	83
8	3300	380	70
11	3000	530	83
14	2200	80	90
18	3070	320	74
21	2800	1200	79
25	3140	900	92
30	5100	2000	90
C.S.I.R. Strain Gage Strain Cell - Borehole No. 3			
4	6800	2900	90
6 ft. 11 in.	5000	2200	110
10 ft. 1 in.	3200	145	98
12 ft. 5 in.	3400	185	103
13 ft. 2 in.	2900	670	90
15	3400	600	102
19	2950	-110	84

Results obtained in three boreholes drilled in 14 extension drift. (Van Heerden and Grant)

calculated. The results were evaluated using statistical techniques with a computer program. As might be expected, the flat jack stress values were more than twice that found by the doorstoppers since the flat jacks could only be used very near the mine opening. The doorstoppers conversely were used at some depth, which should have approached virgin rock conditions. The ratio of $S_1:S_2:S_3$ for the two methods was in very good agreement. The value of S_1 (vertical stress) found with the doorstopper is close to the gravity overburden stress. For these studies Stephenson and Murray used stress concentration factors $a = 1.53$, $b = 0$, and $c = -1.0$. It is interesting to note that the measured horizontal stresses are higher than the vertical stresses. The final statistically averaged stress values are given in table 2.7.

Capozza, Martinetti and Ribacchi (16) made measurements in pillars of an Italian marble quarry using both doorstoppers and the USBM borehole deformation gage. Comparative measurements were made in one pillar by placing the two gages in parallel holes about 2 meters apart. For stress concentration factors, the results given by Hiramatsu and Oka (9) and those given by Van Heerden (8) were used separately to yield two different sets of stress values. The component of stress parallel to the borehole axis was assumed to be zero. The comparison of results is rather poor. Capozza postulated that the difference was probably due to assuming that the stress parallel to the borehole axis was zero,

TABLE 2.7

Stress component	Borehole value (psi)	Flat jack value
S_1	1627	3800
S_2	1661	3200
S_3	1160	2400

Comparison of borehole and flat jack measurements of vertical and horizontal stress components on the 1200 ft. level. (Stephenson and Murray)

and that this assumption had dissimilar effects on the two different gages. It is felt unlikely that this argument is valid, since measurements taken so near to the free face of the pillar should not be affected by any significant stress parallel to the borehole. Observe the results in table 2.8.

Bonnechere and Fairhurst (17) compared a number of stress measuring instruments under simulated field conditions. Their method was to cut a 4-1/2 foot square block of granite loose from a quarry floor by drilling overlapping holes along its periphery. Flat jacks were then installed on all four sides of the block to simulate a field stress. The various instruments were installed on the surface of the block and into boreholes drilled into it. Among the various devices tested were several doorstopper gages and a borehole deformation gage designed by Crouch. This borehole deformation gage is very similar to the USBM gage, but measures deformations on four diameters rather than three. For purpose of comparison the maximum principal strain indicated by each instrument was calculated. Using the measured strains and the known applied stress, Young's modulus was calculated. Table 2.9 shows the results of several uniaxial compression tests. Doorstoppers mounted on borehole bottoms and the borehole deformation gage only are considered.

Bonnechere and Fairhurst used stress concentration factors for the borehol bottom of $a = 1.25$, $b = 0$ and assumed the axial

TABLE 2.8

depth	ϕ	S_1 kg/cm^2		S_2 kg/cm^2		method
1.7m	81°	120*	120**	40*	15**	doorstopper
2.5m	80°	135*	135**	25*	0**	
0.3-1.5m	76°	170		50		borehole deformation gage

* - by Hiramatsu and Oka

** - by Van Heerden

ϕ is measured from horizontal to S_1

Results of stress measurements in Italian marble quarry.

(Capozza, Martinetti and Ribacchi)

TABLE 2.9

Stress Direction	Gage	Principal strain (at 1000 psi)	E 10^6 psi
E-W	Doorstopper #1	151	6.6
	Doorstopper #2	134	7.5
	Borehole deformation	148	6.8
N-S	Doorstopper #1	124	8.1
	Doorstopper #2	163	6.1
	Borehole deformation	168	6.0

Comparison of doorstopper and borehole deformation gage in granite block after Bonnechere and Fairhurst.

stress to be zero. As can be seen, there is quite a bit of spread in the data, and even between the two doorstoppers. It is of interest to note that the average values of the two doorstoppers in the E-W direction is nearly the same as for the N-S direction. Bonnecherre and Fairhurst conclude by saying that the results of the experiment show that any one reading by a stress determining instrument should not be trusted by more than 20-30%.

3. FINITE ELEMENT STUDY

3.1 Introduction

A finite element study of the stresses on a flat borehole end was made for the purpose of comparing the results with the experimental data obtained in the Colorado School of Mines experimental mine.

The finite element sudy is based on an axisymmetric program for purposes of simplification. With this technique, the borehole and surrounding rock are considered to be concentric cylinders of finite size. This allows the construction of a nodal point array on a single axial plane (actually a half plane). Pressure is applied on this plane axially for the determination of SCF c and radially for the determination of SCF a and b. The computer program then rotates the applied pressure and nodal point array about the axis of the borehole, generating a uniform radial or axial pressure and a system of nodal circles and ring elements.

Since the axisymmetric program, with applied radial pressure, generates a uniform radial stress field about the borehole axis, it is impossible to separate the stress concentration factors a and b. Only their sum may be determined. This fact was pointed out by Coates (11, 18). If one assumes that b is equal to zero, as did Crouch, then a may be determined. There is much justification for this assumption as most researchers have found b to be zero or very near to zero. If b is not equal to zero then

the values of SCF a published by Crouch are most likely the sum of a+b, since he used an axisymmetric program.

3.2 Presentation of Results

To calculate values of the stress concentration factors for the flat borehole end, the radial stress in the eight elements forming the radius of the borehole end are considered. These radial stresses were divided by the applied pressure to yield the stress concentration factors for values of Poisson's ratio of 0.1, 0.2, 0.3, and 0.4. The variations of the stress concentration factors across the borehole end are plotted in figs. 3.1 and 3.2.

The strain gage rosette used in the experimental part of this research would measure radial strains over only the area represented by the first two elements from the borehole axis. The average stress concentration factors of these two elements is used for comparison with experimental data. Table 3.1 lists the results obtained. These values are also plotted in figs. 3.3 and 3.4 along with values published by Coates and Yu (11) and Crouch (10).

3.3 Discussion of Results

The finite element technique is, of course, only an approximation. This fact is pointed out by the diverse results obtained from the finite element studies of Crouch, Coates and the author in analyzing the same relatively simple problem.

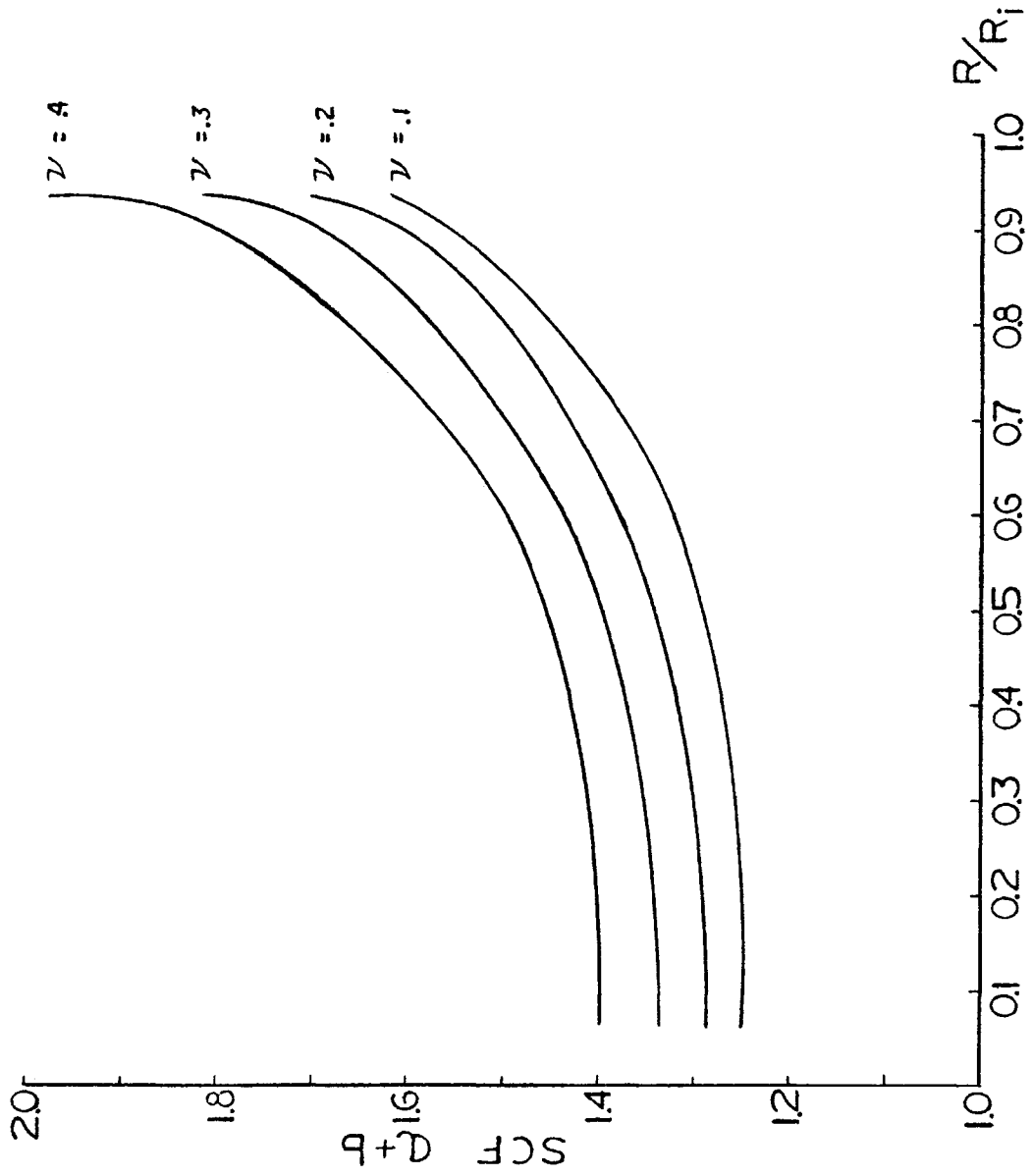

fig. 3.1 Variation of SCF a+b across the borehole end.

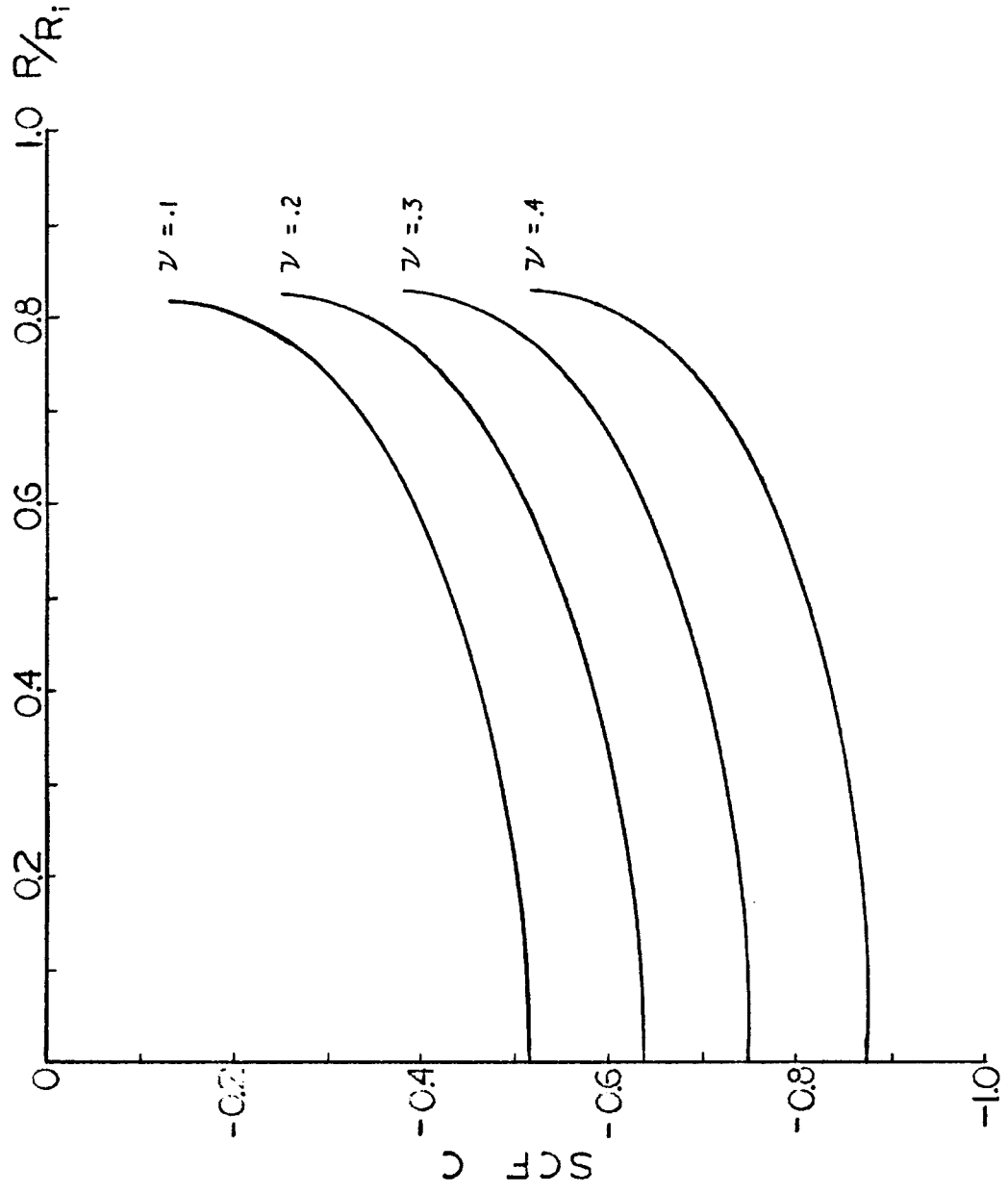

fig. 3.2 Variation of SCF c across the borehole end.

TABLE 3.1

Poisson's ratio	a + b	c
0.1	1.25	-0.51
0.2	1 29	-0.63
0.3	1 34	-0.75
0.4	1 40	-0.87

Stress concentration factors determined from finite element study.

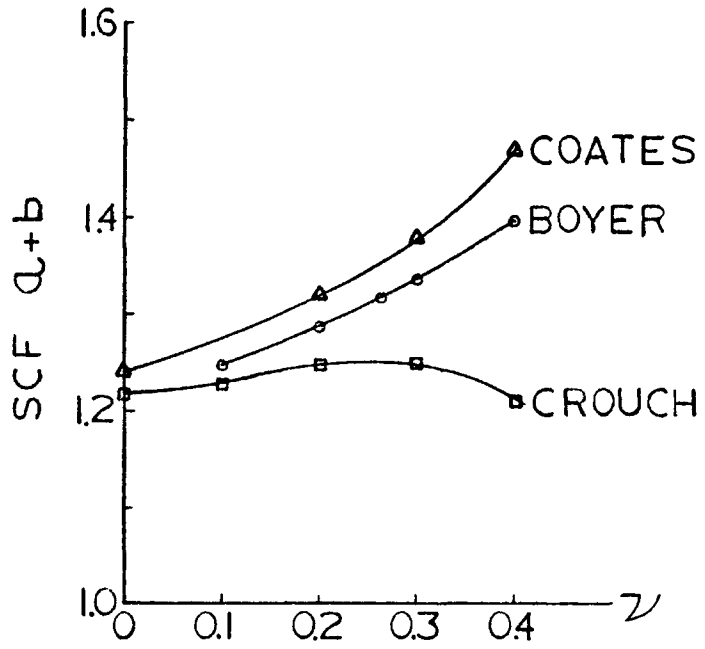

fig. 3.3 Variation of SCF a+b with Poisson's ratio (ν). Finite element studies.

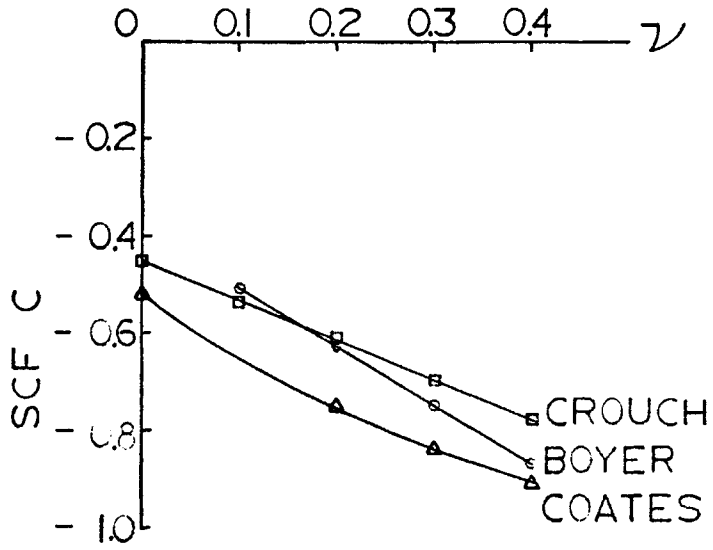

fig. 3.4 Variation of SCF c with Poisson's ratio (ν). Finite element studies.

Among other things, the results from a finite element study are affected by the complexity of the element array, the computer program, the method of application of boundary forces, the restrictions placed on the model and by interpretation of the print-out.

It is not the intent here to discuss these various problems with the exception of the method of print-out interpretation. The computer program results in a print-out of the stresses in each element of the array, and these stresses are considered to be at the element's centroid. Since the flat end of the borehole is formed by the edges of a row of elements, the stresses on the borehole end are not necessarily those at the centroid of the elements forming the borehole end. Because of this, it is necessary to extrapolate the stresses to the borehole end.

The extrapolation was accomplished by plotting the radial stresses in each column of elements parallel to the borehole axis and immediately beyond the borehole end. For a radial applied boundary pressure, the stress gradient in these element columns was very small. It was found that accepting the radial stress value in the elements forming the borehole end as the stress on the borehole end would result in an error of less than 1%. Thus no extrapolation was necessary in this case.

For an axial applied boundary pressure, however, the situation was very different. The radial stress in element columns

parallel and near to the borehole axis decreased exponentially beyond the borehole end. Thus it was required to extrapolate the distance of 1/2 element from the centroid of the row of elements forming the borehole end to the borehole end. This was done by plotting the radial stresses on semi-log paper and extrapolating graphically. The radial stresses in the element columns near the borehole axis plotted to a straight line on semi-log paper, and it was assumed that the function was continuous to the borehole end. Compare figs. 3.2 and 3.5 for the difference in stress concentration between borehole end and the row of elements forming the borehole end.

By methods of curve fitting, mathamatical relationships between the stress concentration factors and Poisson's ratio were determined. These equations are:

$$a + b = 1.2e^{.385\nu}$$

$$c = -0.39 - 1.2\nu$$

It is interesting to note that values of $a+b$ predicted by the three finite element studies under discussion are similiar for $\nu = 0$, but diverge widely from there. For comparison sake, these values are re-tabulated in table 3.2.

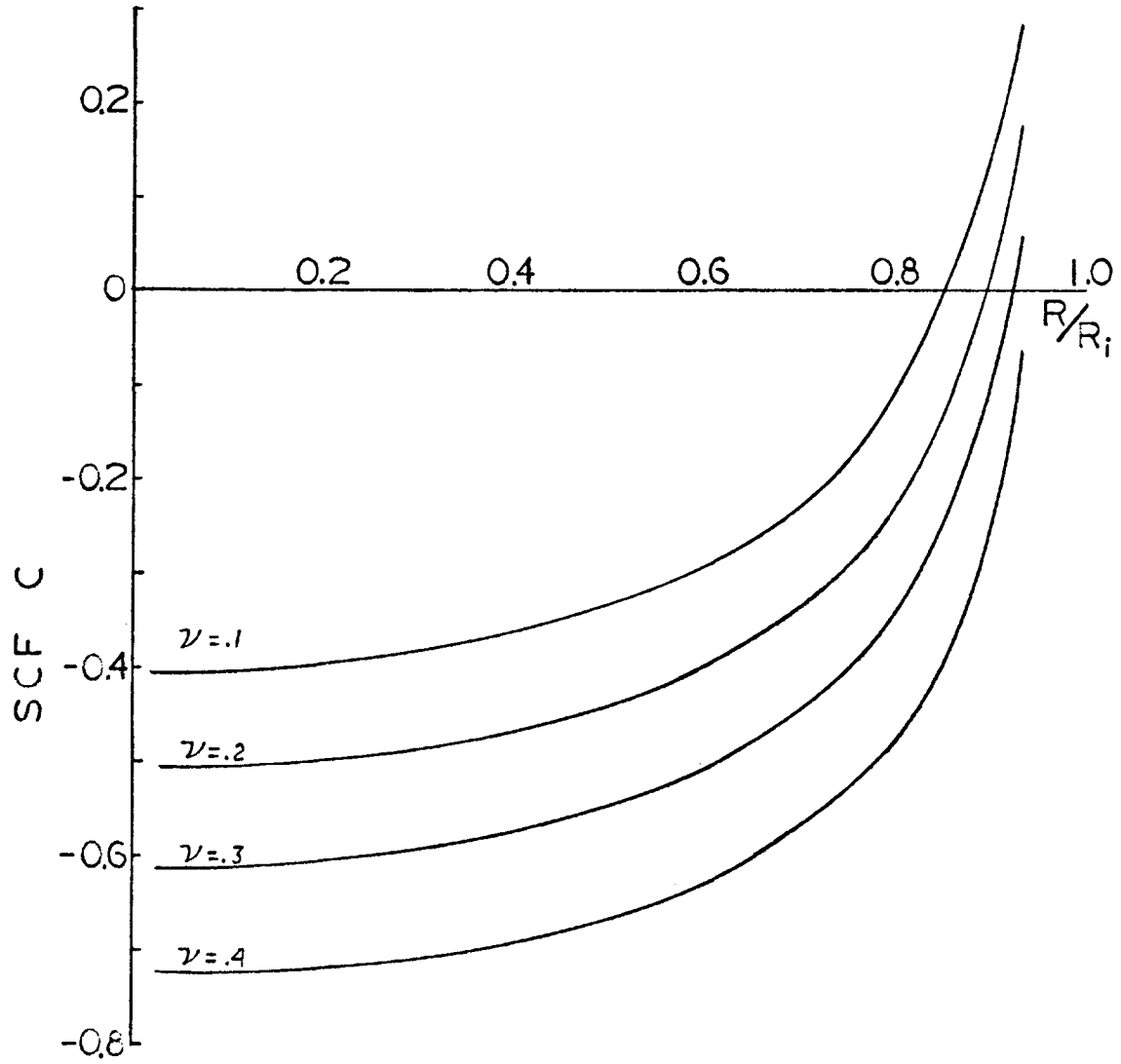

fig. 3.5 Variation of SCF c across the row of elements adjacent to the borehole end.

TABLE 3.2

Poisson's ratio	a+b Crouch	a+b Coates	a+b Boyer	c Crouch	c Coates	c Boyer
0.0	1.22	1 24	1.20	-0.46	-0.52	-0.39
0.1	1.23	1.27	1.25	-0.54	-0.64	-0.51
0.2	1.25	1.32	1.29	-0.62	-0.75	-0.63
0.3	1.25	1.37	1.34	-0.70	-0.84	-0.75
0.4	1.21	1.45	1.40	-0.78	-0.91	-0.87

Stress concentration factors predicted by several finite element studies.

4. EXPERIMENTAL RESULTS

4.1 Introduction

The use of a doorstopper gage permits the calculation of stress by measuring strains on the end of a borehole. These measured strains are reduced to the principal stresses on the borehole end by equations derived from elastic theory. The strain rosettes used here were the equiangular type, measuring radial strains at 60 degree intervals. These strains are designated:

ϵ_1 0°

ϵ_2 60°

ϵ_3 120°

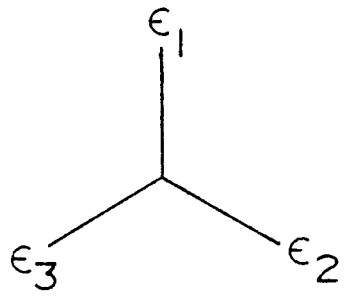

with the ϵ_1 strain being aligned with some fixed reference. In this case ϵ_1' is aligned with one of the applied flat jack loads. This direction is designated the X direction. The Y direction is perpendicular to X and in the plane of the borehole end. The Z axis is down the center of the borehole.

To obtain the principal stresses on the borehole end, the principal strains and their orientation are calculated by:

$$\epsilon_{max} = \frac{\epsilon_1 + \epsilon_2 + \epsilon_3}{3} + \frac{\sqrt{2}}{3} \sqrt{(\epsilon_1 - \epsilon_2)^2 + (\epsilon_2 - \epsilon_3)^2 + (\epsilon_3 - \epsilon_1)^2}$$

$$\epsilon_{min} = \frac{\epsilon_1+\epsilon_2+\epsilon_3}{3} - \frac{\sqrt{2}}{3}\sqrt{(\epsilon_1-\epsilon_2)^2+(\epsilon_2-\epsilon_3)^2+(\epsilon_3-\epsilon_1)^2}$$

$$\phi = \frac{1}{2}\,\mathrm{TAN}^{-1}\,\frac{\sqrt{3}\,(\epsilon_2-\epsilon_3)}{2\epsilon_1-\epsilon_2-\epsilon_3}$$

where ϕ is the counter-clockwise angle from ϵ_1 to ϵ_{max}. The principal stresses on the borehole end may then be calculated by:

$$\sigma_{max} = \frac{E}{1-\nu^2}\,(\epsilon_{max}+\nu\epsilon_{min})$$

$$\sigma_{min} = \frac{E}{1-\nu^2}\,(\epsilon_{min}+\nu\epsilon_{max})$$

where E is Young's modulus and ν is Poisson's ratio.

The experimental work in this project consisted of applying known uniaxial and uniform biaxial loads to a block of Indiana limestone equipped with a doorstopper gage. The equipment and techniques used are described in appendicies A and B of this work. The applied stresses are assumed to be the principal stresses in the rock. The principal stresses on the borehole end are calculated from doorstopper measured strains and are divided by the known applied stresses to obtain stress concentration factors.

Preliminary tests were carried out in small blocks of Indiana limestone, hydrostone, and plexiglass to determine reliability of the gage. Also determined in preliminary experiments were such

factors as bonding pressure, gage alignment and method of testing.

Initial tests were made with uniaxial compression in a Tinius Olsen testing machine. Indiana limestone was chosen for the research program because of its homogeneity, fine grain structure and apparent isotropy. Several six inch cubes of limestone were prepared by drilling a 1-1/2 inch diameter hole, 3 inches deep into the center of one face with a thin wall coring bit. The bottoms of the boreholes were ground smooth with a flat faced diamond bit. After several trials it was found that the use of BLH EPY-150 cement and a bonding pressure of 10 psi gave a satisfactory bond between gage and rock.

From the first tests made a large amount of recoverable creep showed up in the strain readings. It appears that this creep was in the limestone itself or in the cement bond and not in the loading system, as it appeared in the mine testing as well as the preliminary laboratory tests. After much trial and error it was found that the effect of the creep could be nearly eliminated by preloading the speciman for about 5 minutes, removing the load and quickly zeroing the strain indicator, applying the load and recording the strain readings, and returning the load to zero for a final check. With this method the strain readings could be brought back to zero and the inelastic strains eliminated. It was necessary to follow this procedure throughout the project, result-

ing in a great number of load-unload cycles.

4.2 Determination of SCF a and b

Two separate groups of tests were performed for this section. Group I was a set of uniaxial compression tests applied in the ϵ_1 direction. Group II was a set of uniform biaxial compression tests applied in the direction of and perpendicular to ϵ_1. Each group consisted of 10 separate runs, each run consisting of 5 individual sets of strain readings. This resulted in 50 cycles of loading and unloading for each group of tests.

The biaxial tests were performed first. Prior to these tests, the limestone block had been unstressed, and a large amount of non-recoverable creep appeared in the first few stress cycles. For this reason, the fir .t two runs in Group II were discarded as being anomalous.

Results of the Group I tests are presented in table 4.1. The stresses indicated are the principal stresses on the borehole end. As can be seen from table 4.1, the results of Group I tests are fairly uniform and reproducible. The tests indicate a SCF a of 1.29 for the Indiana limestone block which has a Poisson's ratio of 0.224. The value of ϕ should be zero under ideal conditions. Its magnitude provides a check on the accuracy of measurements. The low angle of $2^{\circ}45'$ indicates a good level of accuracy.

The difficult thing to interpret in the Group I tests is the unexpected high value of σ_{min}. Previous research in the doorstopper

TABLE 4.1

Applied load psi	σ_{max} psi	SCF a	ϕ	σ_{min} psi
-500	-667	1.33	2°45'	203
-500	-652	1.31	2°45'	203
-500	-652	1.31	2°45'	203
-500	-633	1.27	3°00'	208
-500	-627	1.25	3°15'	198
-500	-647	1.29	3°00'	208
-500	-662	1.32	2°30'	213
-500	-642	1.28	2°15'	193
-500	-637	1.27	2°30'	188
-500	-627	1.25	2°45'	188
Averages				
-500	-645	1.29	2°45'	202

Group I tests - uniaxial load.

field indicates that the value of σ_{min} should be near zero in a truly uniaxial stress field. Apparently, some degree of lateral restraint was developed in the system resulting in the generation of a stress across the borehole end. The restraint could have come from friction between the block and loading system or could have been the result of non-uniformity in the loading. This problem is discussed more thoroughly in section 4.5. The ratio of σ_{min} to σ_{max} is about -0.31 which could indicate a uniaxial load with a good deal of lateral restraint. Theoretically, complete lateral restraint in the system would result in a ratio of $-\frac{\nu}{1-\nu}$ or -0.29. The high value of σ_{min} could also be interpreted to be the effect of a SCF $b = -0.4$. But this high value of b is inconsistent with all previous research and the author feels such a conclusion is unjustified.

Since the degree of error inflicted by the poor loading system cannot be determined, stress concentration factor b could not be determined.

The results of Group II tests are tabulated in table 4.2. As can be seen from table 4.2, the results from the biaxial tests were not as uniform and reproducible as the uniaxial tests. The much higher and somewhat scattered values of ϕ indicate a more serious error. The values of σ_{min} are so varied as to be meaningless. It is difficult to understand how the values of σ_{max} can be reasonably uniform and the values of σ_{min} so varied. Other

TABLE 4.2

Applied load psi	σ_{max} psi	SCF a+b	ϕ	σ_{min} psi
-500	-628	1.26	-9°45'	-10
-500	-642	1.28	-8°15'	48
-500	-677	1.35	-8°45'	58
-1000	-1342	1.34	-8°45'	-440
-1000	-1190	1.19	-15°30'	-135
-1000	-1295	1.30	-13°45'	-72
-1000	-1290	1.29	-14°45'	-92
-1500	-1792	1.20	-15°30'	-928
Averages				
---	---	1.28	-11°45'	---

Group II tests - uniform biaxial load.

researchers have experienced this problem (14).

The biaxial tests indicate that the average sum of stress concentration factors $a+b$ is 1.28 for the Indiana limestone block. This is so near to the value of $a = 1.29$ indicated by the uniaxial tests that SCF b can probably be assumed to be zero, at least for a Poisson's ratio of 0.224. The finite element study described in section 3. of this thesis predicts a value of $a+b$ as:

$$a+b = 1.2e^{.385\nu}$$

$$1.2e^{.385(.224)}$$

$$1.31$$

This is a fairly good agreement.

4.3 Determination of SCF c

Tests for the determination of SCF c were performed in a similar manner to those for SCF a and b. For the Group III tests, an axial load was applied to the limestone block containing the doorstopper. Theoretically, this axial load should result in a uniform radial stress on the borehole end. Problems in the loading system, however, prevented the radial stresses from being exactly uniform. To obtain the SCF c, the average radial stress on the borehole bottom had to be determined. This could be done by either of two methods: (1) Average the values of ϵ_1, ϵ_2, and ϵ_3 and use this average value for ϵ max and ϵ min. Then compute the uniform radial stress σmax (or σmin) as σave. (2) Use the

actual values of ϵ_1, ϵ_2 and ϵ_3 to compute the actual principal stresses, σmax and σmin. Use the average of the principal stresses as the uniform radial stress, σave.

Both methods result in the same value of the average radial stress, within a few percent. Group III tests consisted of 12 runs, with 5 individual sets of strain readings in each run. Table 4.3 tabulates the results. As can be seen from table 4.3, the Group III tests had excellent uniformity and reproducibility. This is most likely a result of the axial tests being free of the end conditions imposed by the flat jacks in the Group I and II tests. Thick sections of acoustic fibreboard were used at both ends of the limestone block for stress distribution. Space limitations prevented this in the Group I and Group II tests.

The finite element study predicts:

$$c = -0.39 - 1.2\nu$$

$$-0.39 - 1.2(.224)$$

$$-0.66$$

as compared to the measured value of -0.75. This disagreement is probably a result of having to interpolate the radial stresses in the finite element study. See section 3.3.

4.4 Results of USBM Borehole Deformation Gage

4.4.1 Brief Theory of the Gage-- The USBM borehole deformation gage measures deformations of a circular borehole rather than strains as does the doorstopper gage. This is a

TABLE 4.3

Applied load psi	σ_{ave} psi	SCF c
-500	373	-0.746
-500	367	-0.734
-500	375	-0.750
-500	376	-0.752
-500	368	-0.736
-500	368	-0.736
-1000	739	-0.739
-1000	765	-0.765
-1000	753	-0.753
-1000	759	-0.759
-1000	758	-0.758
-1000	757	-0.757
Averages		
---	---	-0.749

Group III tests - axial load.

highly convenient method of stress determination as the deformations can be completely predicted by elastic theory, making a theoretical analysis a fairly simple procedure.

The borehole deformation gage measures deformations of the borehole on 3 diameters in an equiangular pattern. These deformations are designated:

U_1	0°
U_2	60°
U_3	120°

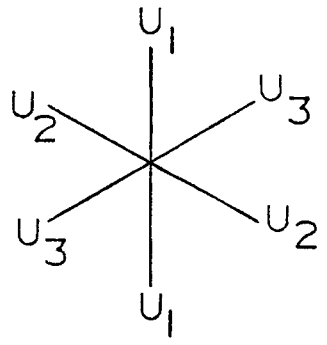

Equations have been derived which calculate the principal stresses directly from the values of U_1, U_2 and U_3. See references 19 and 20. The principal stresses and their orientation are calculated by:

$$\sigma_{max} = \frac{E}{6d}\left[U_1+U_2+U_3+\frac{\sqrt{2}}{2}\sqrt{(U_1-U_2)^2+(U_2-U_3)^2+(U_3-U_1)^2}\right]$$

$$\sigma_{min} = \frac{E}{6d}\left[U_1+U_2+U_3-\frac{\sqrt{2}}{2}\sqrt{(U_1-U_2)^2+(U_2-U_3)^2+(U_3-U_1)^2}\right]$$

$$\phi = \frac{1}{2}\,\mathrm{TAN}^{-1}\,\frac{\sqrt{3}\,(U_2-U_3)}{2U_1-U_2-U_3}$$

where d is the borehole diameter and plane stress is assumed.

Plane strain may also be assumed which results in a mod-

ification of the equations above and a difference in stress calculated of about 6% under ordinary conditions. Plane stress is assumed for the work in this investigation because of the simplification resulting, and because it probably more nearly represents the actual conditions involved.

4.4.2 Results from the USBM Gage-· The USBM gage was submitted to the same test groups as was the doorstopper gage, with the exception of Group III. It was found that the axial loads had so little effect on the gage that determinations were impossible. The other two groups were done in the same sequence and as discussed in sections 4.2 and 4.3. Table 4.4 tabulates the results of the uniaxial tests. This group of tests gave excellent uniformity and reproducibility. The small values of ϕ and σ_{min} indicate a high degree of accuracy in the measurements. The reason for the 12.4% error is unknown. All equipment used was double-checked for accuracy and no errors could be found. The calibration of the gage was checked and confirmed. Some possible, but unconfirmed, sources of error are (1) The assumption of plane stress, (2) Variation in borehole diameter, (3) Inclination of borehole, (4) Eccentricity of the borehole, (5) Non-uniform leading, (6) Variations in Young's modulus.

The results of the biaxial tests are tabulated in table 4.5. Paralleling results with doorstopper measurements, the biaxial tests show more dispersion and somewhat poorer results than

TABLE 4.4

Applied load psi	σ_{max} psi	σ_{min} psi	ϕ
-500	-543	-30	1° 15'
-500	-548	-31	1° 30'
-500	-546	-36	1° 30'
-500	-578	-35	2° 30'
-500	-577	-34	2° 15'
-500	-582	-34	2° 15'
-500	-557	-32	2° 15'
-500	-565	-36	2° 30'
-500	-566	-34	2° 15'
-500	-560	-32	2° 15'
Averages			
-500	-562	-33	2° 00'
σ_{max} average error	12.4%		

Group I tests - uniaxial load - borehole deformation gage.

TABLE 4.5

Applied load psi	σ_{max} psi	σ_{min} psi	ϕ
- 500	- 548	-29	-4°15'
- 500	- 562	-30	-5°15'
- 500	- 565	-27	-5°30'
- 500	- 568	-32	-6°15'
-1000	-1126	-37	-4°45'
-1000	-1136	-43	-4°30'
-1000	-1175	-58	-4°45'
-1500	-1578	-20	-6°30'
Averages			
---	---	---	-5°15'
σ_{max} average error	12.2%		

Group II tests - uniform biaxial load - borehole deformation gage.

the uniaxial tests. Again the value of σ_{min} is unexplainable, and values of ϕ are larger. The average error in σ_{max} is, however, nearly the same as in the uniaxial tests. This leads one to believe that this 12% error is not caused by the loading system, but may be a function of the borehole geometry, a factor which would affect both test groups equally.

4.5 Discussion of Results and Problems

The largest error in all the test groups is in the determination of σ_{min}. During testing, some uniaxial tests were made with applied load in the Y direction, or perpendicular to the ϵ_1 - U_1 direction. These tests resulted in a fair value for σ_{max}, but indicated a value of ϕ that was about 30 degrees off. Thus it was suspected that something was wrong with the loading in this direction.

To confirm the suspicion, photoelastic discs were glued to the top of the limestone block to provide a visual, qualitative estimate of the uniformity of stress distribution in the block. With an applied uniaxial load in the X direction, the fringe patterns were nearly the same in all the discs, indicating a fair uniformity. With uniaxial loading in the Y direction, the fringe patterns were elongated in several directions in the different discs. With a uniform biaxial load, the fringe patterns appeared to be somewhere between the results of the two different uniaxial loads.

The photoelastic checks indicated that something was indeed

wrong with the Y axis loading system. It appears that the system of shims used for filling in gaps between test block and hole resulted in semi-point loading and a non-uniform stress distribution in the block. This, it is believed, is the reason for the unexplainable values of σ'_{min}, and for the poorer general results in the biaxial tests. The use of both flat jacks together apparently lessened the effects of the poor loading in the Y direction, so that some of the results are reasonable. Methods of reducing this type of error are discussed in Appendix A of this work.

By way of comparison between the doorstopper and the borehole deformation gage, it can be seen that the borehole deformation gage gave more favorable results under the poor loading situation, even if there is an apparent error of 12%. It is impossible to determine the amount of error in the doorstopper measurements since the stress concentration factors are to be determined. The borehole deformation gage has very little sensitivity to axial loads, which is a definite advantage.

5. CONCLUSIONS

The major conclusion of this work is to present a set of stress concentration factors for doorstopper use which are substantiated by both the finite element study and the experimental work. Because there is some disagreement in the two methods, some modifications have been made.

First, since experimental determinations of $a+b$ are very close to that predicted by the finite element study, the function proposed in section 3.2 for $a+b$ will be accepted.

Second, experimental work indicated that the value of $a+b$ was very near to the value of a, or in other words $b=0$ for practical purposes. Thus the function for $a+b$ becomes the function for a.

Third, experimental determination of SCF c gave such excellent results that it is felt they should be used to modify the function for c suggested in section 3.2. This function was found by extrapolation and it appears that this resulted in values of c which are slightly low. The function is a first degree equation, and is a straight line. Since the extrapolation of radial stresses was the same for all points on the line, the slope of the line should be correct. It is only necessary then to adjust the intercept of the line to force it through the point $c=-0.75$ rather than $c=-0.66$ for a Poisson's ratio of 0.224.

The proposed functions for the stress concentration factors

then are:

$$a = 1.2e^{.385\nu}$$

$$b = 0$$

$$c = -0.48 - 1.2\nu$$

Table 5.1 is a tabulation of values indicated by these functions for various values of Poisson's ratio. These values are similar to values found by earlier research (8,9,10,11), but again there is no definite agreement. This fact points out the major drawback to the use of doorstopper gages. The use of stress concentration factors found by experimental work is subject to all the errors inherent in working with a medium such as rock. A rigorous theoretical solution as a base for all experimental work is needed.

The borehole deformation gage is not encumbered with the problems of interpretation that exist with the doorstopper. This makes the deformation gage the logical choice where high accuracy is needed or complex stress fields are involved.

The doorstopper can be effectively used for simple problems such as pillar stress determinations, or where much is known about the type and direction of stress field involved, or where only rough measurements are desired.

TABLE 5.1

Poisson's ratio	a	b	c
0	1.20	0	-0.48
.1	1.25	0	-0.60
.2	1.29	0	-0.72
.3	1.34	0	-0.84
.4	1.40	0	-0.96

Final SCF determined in this work.

APPENDIX A

Design and Construction of the Testing Machine

Introduction

The original concept for this research work included an attempt to approach actual field conditions as nearly as possible. For this reason, the testing equipment was designed for installation underground in the Colorado School of Mines experimental mine at Idaho Springs, Colorado. This experimental set up had several important advantages:

1. Use of equipment in actual mining environment.
2. Elimination of need for large and costly support structure to withstand thrust reactions.
3. Constant temperature conditions.
4. Isolation of work area from interrupting influences.

The set up also had several important drawbacks:

1. Inaccuracies introduced by using a roughly shaped mine drift as an intregal part of the test machine.
2. Dust.
3. High humidity.
4. Blasting damage.
5. Difficulties in moving and installing equipment.
6. Restricted space.

Design concept

The testing machine was conceived as one which would be

able to apply compressive stresses on a block of rock in three mutually perpendicular directions. It was desired to be able to vary these applied stresses independently of one another. This is somewhat the reverse of the actual field use of doorstopper gages where the stresses in the rock (normally compressive) are relieved by overcoring.

The block of rock, which was to contain the doorstopper gage and the USBM gage, was to be as large as possible to handle conveniently in order to avoid end effects. It was decided that a block approximately 12 inches square by 30 inches long would meet the requirements. The borehole would be drilled in the center of the 12x12 face to a depth of 15 inches. This borehole would contain the doorstopper on its flattened end and the USBM borehole deformation gage far enough back to avoid restraint from the borehole end. With this configuration, both gages should be subject to exactly the same field stresses, making a very accurate comparison possible.

Machine Construction

A short dead-end drift off of the main entry of the experimental mine was chosen as a suitable site. This area of the mine is located in a very competent gneiss formation and provided an adequately strong rock frame for the test equipment.

To provide a suitable frame for the test block, a hole approximately 5 feet in diameter and 5 feet deep was excavated in the

floor of the drift. A form, for the hole which was to contain the test block, was erected in the center of the excavation. This form provided a hole 12 inches square by 48 inches deep finished size. The excavation was filled with concrete (steel reinforced) and smoothed out to be level with the floor of the drift.

Lateral pressure (perpendicular to the borehole) on the test block was provided by two flat jacks placed on adjacent walls of the test hole. The opposite walls of the test hole then produced restraint for the sides of the block opposed to the flat jacks.

End pressure on the test block was provided by a hydraulic ram of 200,000 lb. capacity. This ram was attached to the roof of the drift directly over the test hole, and pushed vertically on the test block, forcing it against the bottom of the test hole. The ram was anchored to a concrete pad which was secured to the roof with rock bolts.

Construction of the concrete pad was a challenge of its own. Four holes were drilledin the roof on a 16 inch square pattern. Expansion shell bolts were installed, but the standard bolts were replaced by 4 foot lengths of 7/8 inch diameter "all-thread". A one inch thick steel plate was fabricated with a threaded adapter in the center, which would accept the base end of the hydraulic ram. This plate had a one inch diameter hole in each corner to accomodate the four "all-thread" rock bolts. The plate was fitted on the bolts and secured with ordinary hex nuts and flat washers.

A wooden form was built on top of the steel plate. This form was shaped to conform roughly with the contours of the mine roof directly above it. The form was filled with high strength-low slump concrete which was heaped above the sides of the form. The concrete was then forced against the mine roof by tightening the hex nuts supporting the steel plate. With this procedure, the concrete could be forced to conform with roof irregularities, and the steel base plate leveled.

To bridge the gap between ram and test block, a load transfer column was constructed from 10 inch diameter double-extra strong steel pipe. The pipe was fitted with a one inch thick steel plate on either end. A similar, but shorter column was fabricated for the bottom of the test hole to raise the test block to a workable height.

To carry the gage leads out of the hole, a one inch thick steel plate was placed between the test block and the load transfer column. This plate had a 1-1/2 inch deep groove cut from the center hole to one edge. The gage leads were brought out by threading them through the center hole and out the groove.

Discussion

During the actual testing procedure, a number of problems in the equipment design and construction were brought to light.

First, and by far the most serious problem associated with the test equipment was the inaccuracies introduced by misalign-

ment and poor fits. The test hole was shaped with a wooden form which deformed under pressure from the concrete and by soaking up moisture. As a result, the test hole was not precisely shaped. The corners were not square and the distance between opposite sides varied from point to point. This condition necessitated the use of an intricate array of metal shim strips to fill in the gaps between test block and concrete wall, as the flat jacks could not be counted on to deform enough to bridge the gaps. This situation resulted in the generation of point loads on the test block rather than a uniform load over the entire block. Unfortunately, the poor loading system affected the results.

The problems with non-uniform loading could have been eliminated by the use of a heavy metal form, one inch in thickness. This form could be precisely aligned and would not have deformed under pressure from the concrete. The metal form could have been left in place to take some of the flat jack load from the concrete which cracked under very moderate pressures. A system of four flat jacks rather than two should have been used to provide maximum uniformity of loading.

A number of minor problems will be discussed. The end plates of the load transfer column were welded to the pipe, resulting in some warping of the end plates. This was repaired by machining the plates flat, but could have been avoided by the use of threaded fasteners in the first place.

There was a very slight misalignment of the hydraulic ram over the test hole due to the roughness of the mine roof. The base plate for the ram could have been provided with a system for a small amount of lateral movement.

At the beginning of the research project it was planned to test a number of different types of rock with doorstopper gages. However, time did not permit this. The changing of blocks in the hole brought to light another problem. Pressuring the flat jacks caused them to deform around the peripheral weld, wedging the test block, flat jacks and shims very tightly in the hole. They were wedged so tightly, in fact, that the flat jacks and shims could not be pulled out without destroying them. The first test block, which broke during initial testing, had to be removed by breaking it up. In a multi-rock testing program, some system for releasing this residual load would have to be employed.

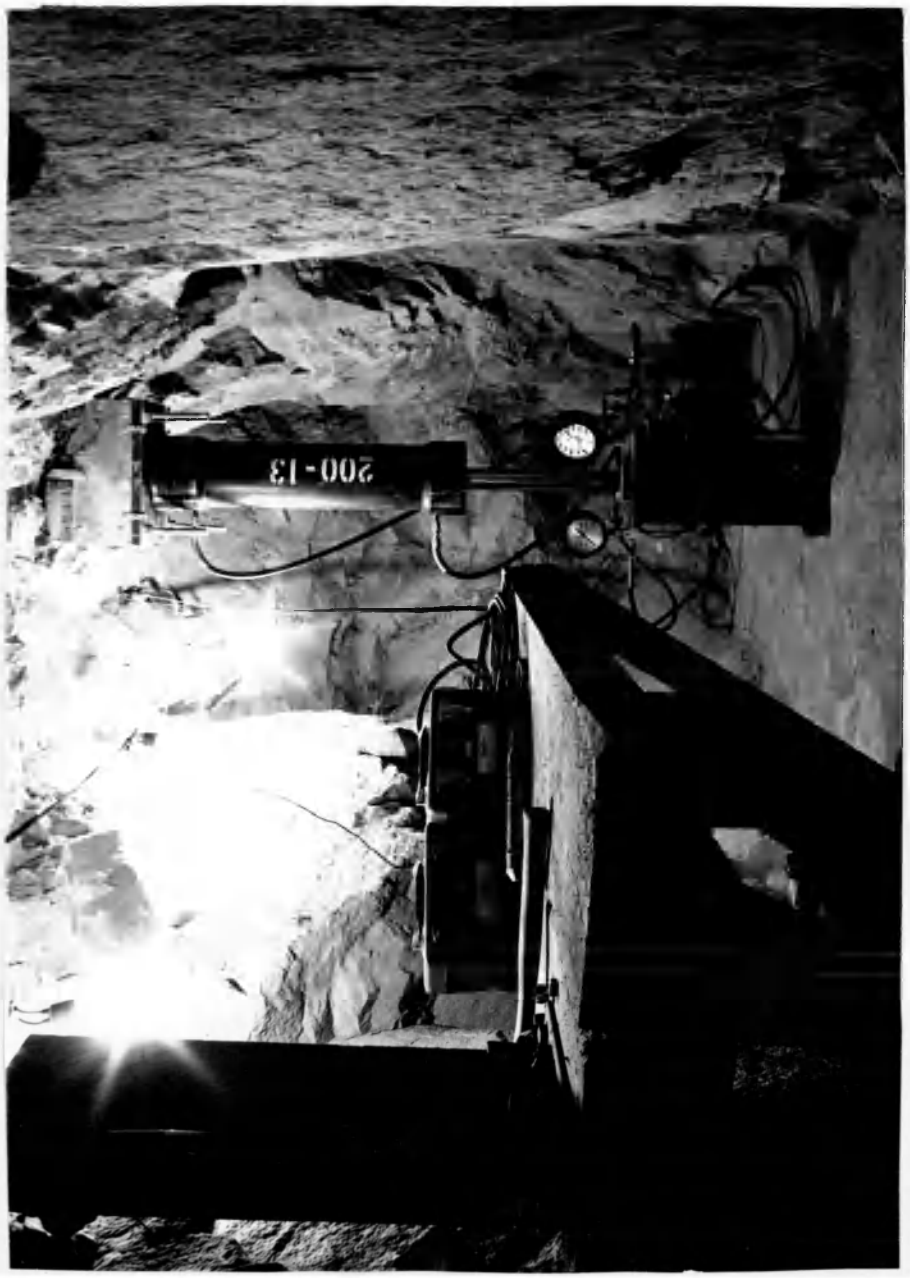

Fig. A.1 - Test site in CSM experimental mine

fig. A.2 - Detail of axial loading system

fig. A. 3 - Detail of axial loading ram

fig. A.4 - Detail of hydraulic system

fig. A. 5 - Detail of load transfer column mounted in test hole

fig. A. 6 - Detail of test hole showing limestone block with gage leads

fig. A. 7 Detail of testing set-up

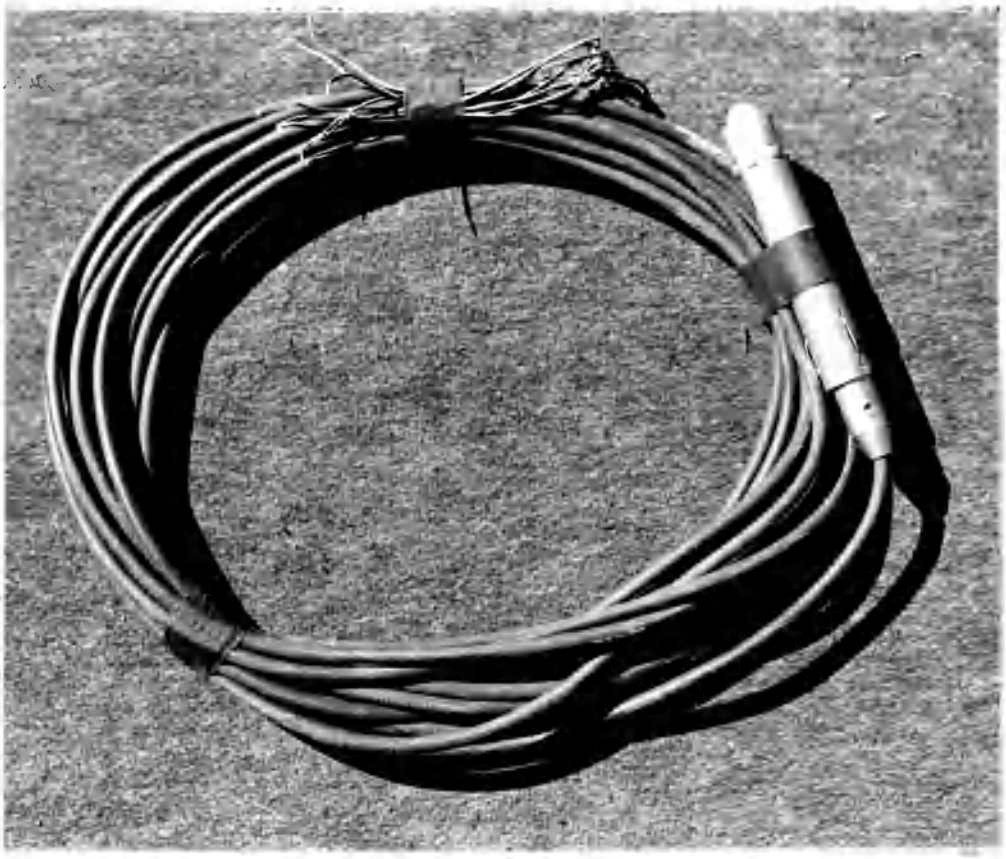

fig. A. 8 USBM borehole deformation gage

fig. A. 9 Budd strain indicator and switch and balance unit

APPENDIX B

Design and Construction of Doorstopper Gage for 1-1/2 inch Hole

Introduction

Doorstoppers designed for a 2-3/8 inch diameter hole are available in South Africa. To the best of the author's knowledge, these are the only available commercially made doorstoppers. To adapt the doorstopper to a 1-1/2 inch diameter hole, it was necessary to come up with a new design which would adapt easily to the required size and which could be made with simple materials and tools available in the Colorado School of Mines mining research laboratory.

Design Concept

A strain gage rosette had to be chosen which would be within the area of uniform stress concentration on the borehole end, but yet large enough to bridge the small irregularities in the rock. For this, an equiangular rosette was chosen, having a diameter of 1/4 inch. This gage would measure strains over the center 1/6 of the borehole end, certainly within the area of uniform stress concentration.

Since the gage would be used for repeated testing, not over-coring, it would be equipped with lead wires rather than the connecting pins found on ordinary doorstoppers. The rosette and the lead wires must then be joined within a holder which would

provide sufficient strength and protection for the delicate connections.

Gage Construction

Early experiments with the same potting compounds used in the construction of the South African doorstoppers proved this method to be unsatisfactory for the small size gage needed. Thus it was decided to eliminate the need for potting-in the rosette.

To provide a low-modulus backing for the strain gage, the rosette was attached to a 7/8 inch diameter by 1/8 inch thick disc of rubber. This assembly was strengthened by attachment to a 7/8 inch diameter by 1/4 inch thick disc of acrylic plastic. Six small holes (#50) were drilled through the disc assembly to accomodate the foil leads from the rosette. Several doorstoppers were constructed by soldering lead wires directly to the foil rosette leads. This method resulted in at least one broken lead in each gage. The problem was solved by the use of connecting pins between the foil leads and wire leads. The tapered connecting pins were inserted into the foil lead holes and wedged tight. The foil leads were then soldered to the pins as were the wire leads. The whole assembly was then strengthened by covering with silicone rubber, which hardened in a few hours. The strain gage assembly was housed in a 2 inch length of 1 inch o.d., 7/8 inch i.d., acrylic tubing. The plastic parts were joined with epoxy cement. The strain gage assembly was mounted so that the outside surface of

the rubber disc was flush with the edge of the outside tubing. This enabled the tubing to be cemented to the rock as well as the strain gage. Any physical disturbance of the gage housing then would not be transmitted to the strain gage grid.

Preparation of the Test Block

The blocks of Indiana limestone for mine testing were diamond sawed to a finished size of 11-1/4 inches by 11-1/4 inches by 36 inches. A 6 inch thick slab was cored in the directions of the three applied stresses in order to determine the degree of anisotropy as well as Young's modulus and Poisson's ratio.

Three inch lengths of 1-1/2 inch diameter core were used for property testing. Each core was equipped with 4 strain gages, two longitudinal and two transverse, mounted at the midplane of the core. The stress-strain curves obtained were very nearly linear, and a tangent modulus was determined. Twelve cores were cut from the first block (which broke during initial testing), four cored in each of the three principal stress directions. The values of Young's modulus and Poisson's ratio obtained from these cores had a small spread. For this reason, and for lack of time, only six cores were taken from the second block, 2 in each of the three principal stress directions. The results from the core testing are tabulated in table B.1.

As can be seen, the block is not completely isotropic, but can be considered to be without introducing any significant

error. The elastic constants were taken as averages over the loading curve from no load to approximately 50% of the compressive strength. The test block had a compressive strength of about 6000 psi and a direct tensile strength of 600 psi.

TABLE B-1

Core	Direction	$E(10)^6$ psi	ν
1	X	4.56	0.222
2	X	4.70	0.243
3	Y	4.37	0.212
4	Y	4.38	0.194
5	axial	4.63	0.231
6	axial	4.88	0.242
Averages			
---	---	4.58	0.224

Results of elastic property tests on Indiana limestone block.

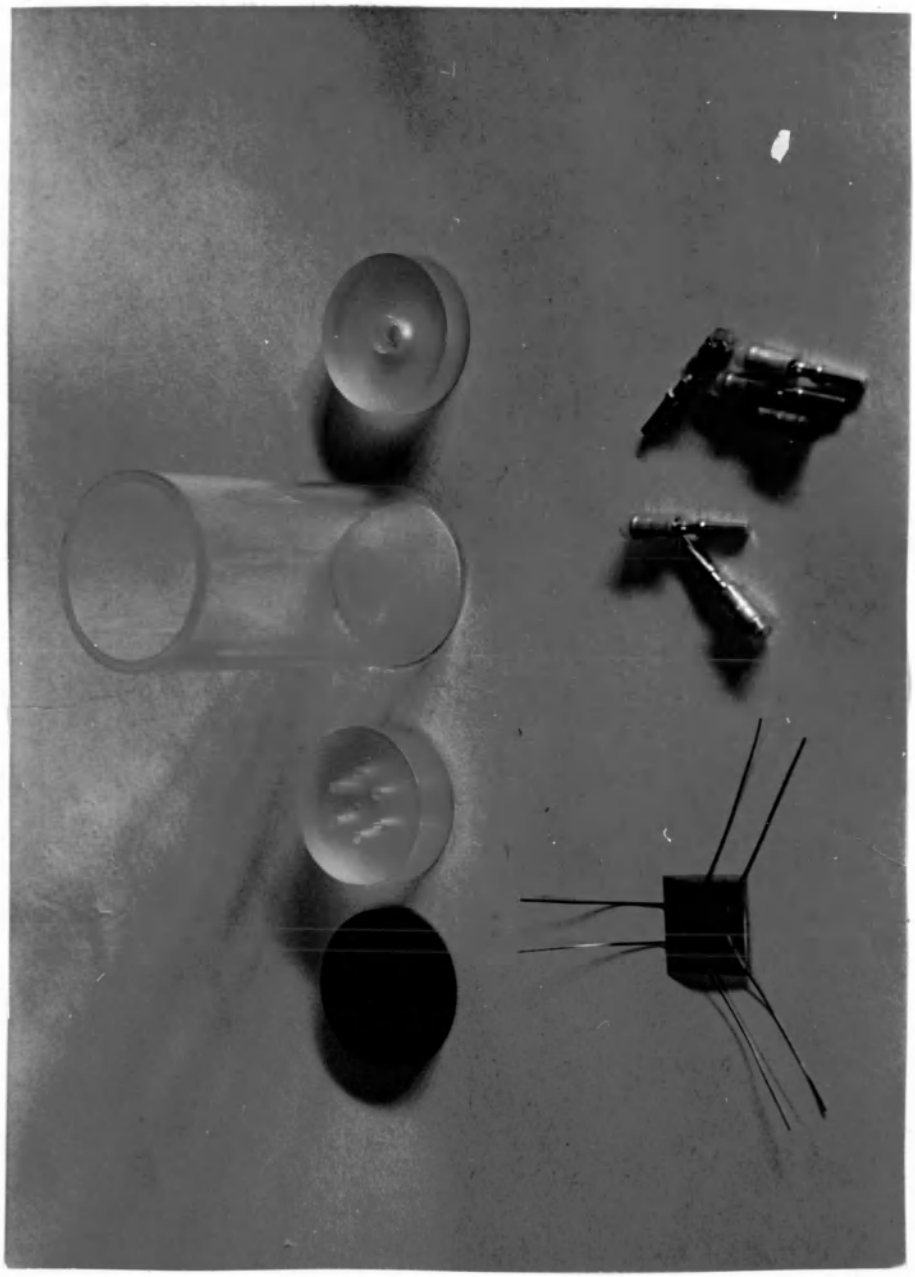

fig. B.1 - Components of the doorstopper gage

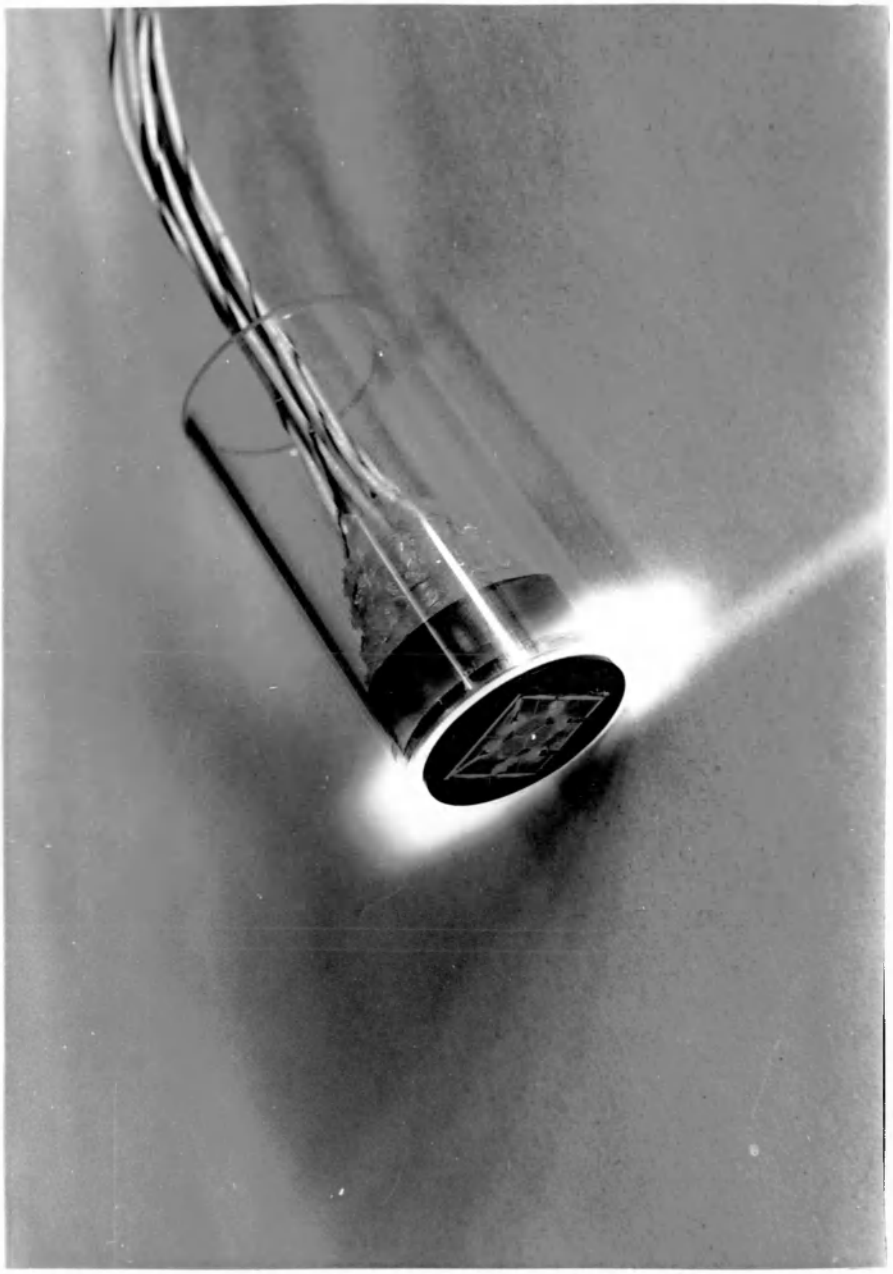

fig. B.2 - Assembled doorstopper gage

APPENDIX C

Fininte Element Program for Analysis of Stress at Borehole End

The following pages contain explanatory information and a computer program furnished by Dr. Wilson Blake of the United States Bureau of Mines Denver Research Center. This material was used for the finite element study appearing in section 3. of this thesis.

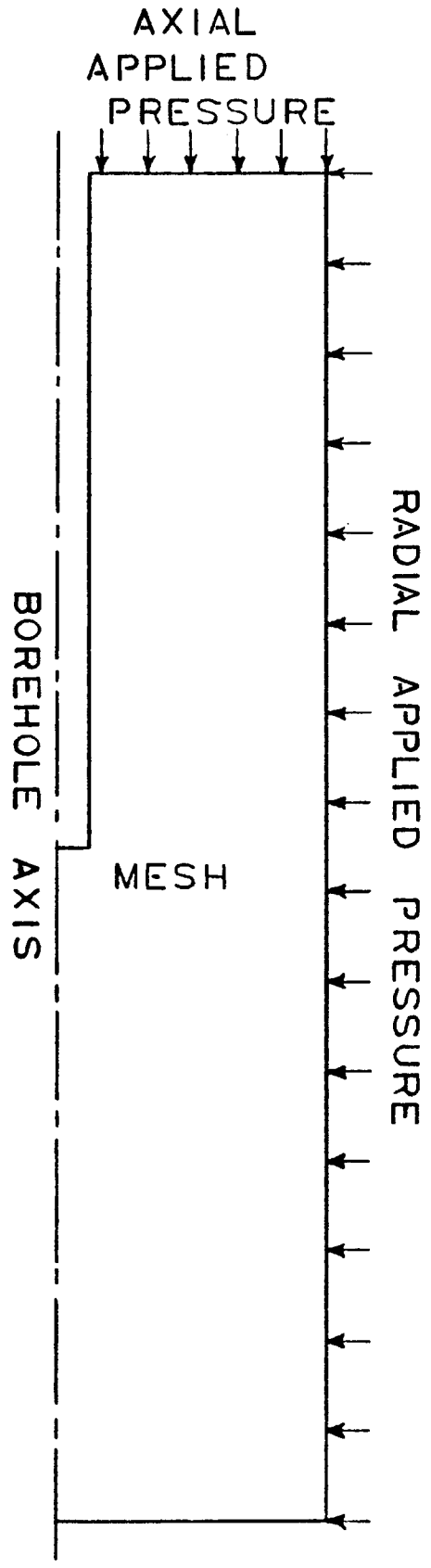

fig. C. 1 Diagram of mesh plan for the finite element program

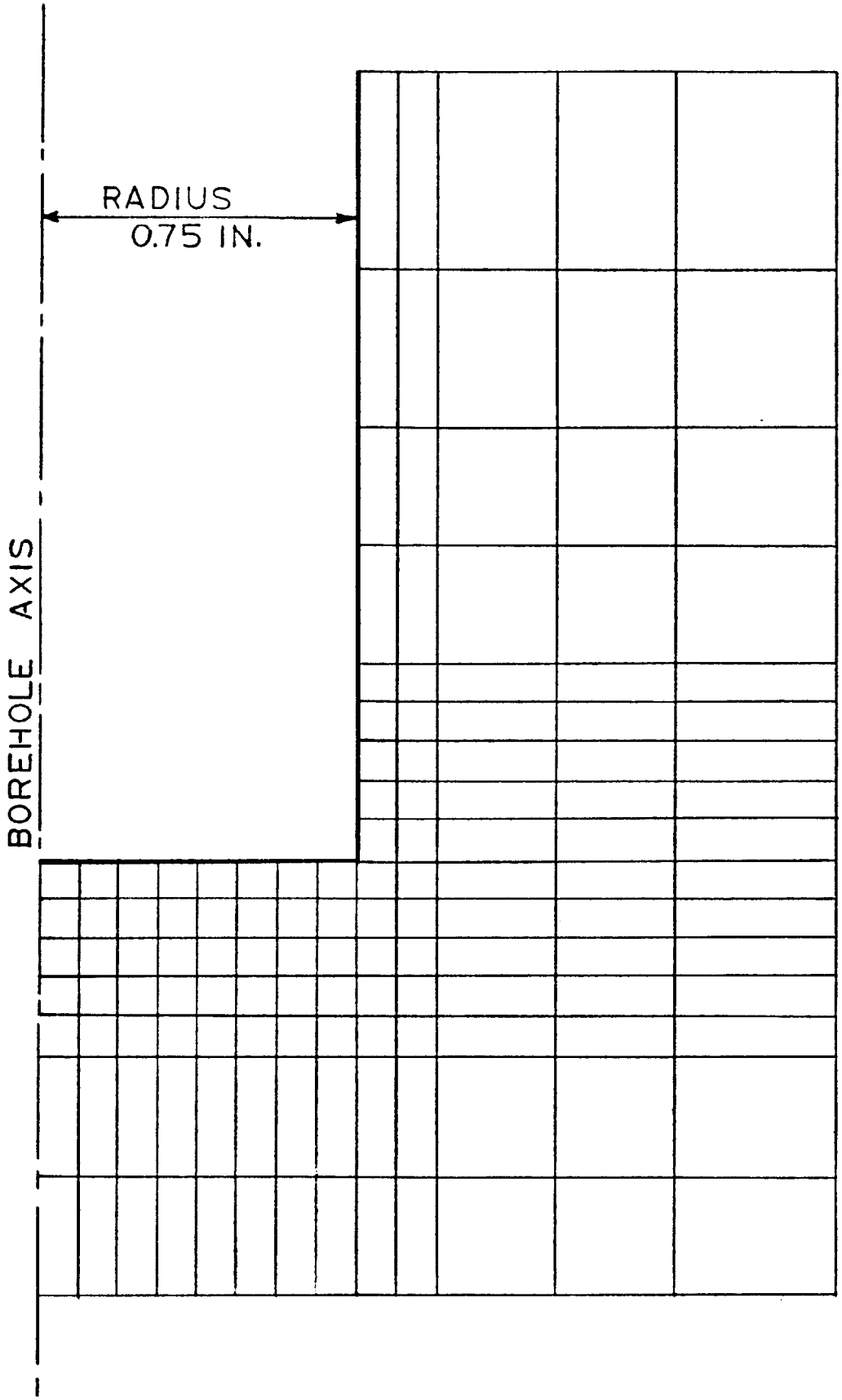

fig. C.2 Detail of element array around the borehole end

UNIVERSITY OF CALIFORNIA
Computer programming series

IDENTIFICATION:

ANALYSIS OF AXISYMMETRIC SOLIDS
Programmed - E. L. Wilson
University of California, February 1967

PURPOSE:

The purpose of this computer program is to determine deformations and stresses within axisymmetric structures of arbitrary shape. The effects of displacement or stress boundary condition, concentrated loads, gravity forces and temperature changes are included. In addition, non-linear material properties are included by a successive approximation technique.

COMPUTER PROGRAM INPUT:

The first step in the structural analysis of an axisymmetric solid is to select a finite element representation of the two-dimentional cross-section of the body. Elements and nodal points are then numbered in two numerical sequences each starting with one. The following group of punched cards numerically define the two-dimensional structure to be analyzed.

A. IDENTIFICATION CARD - (72H)
Columns 1 to 72 of this card contain information to be printed with results.

B. CONTROL CARD - (4I5, 3F10.2, I5)
Columns 1-5 Number of nodal points (900 maximum)
6-10 Number of elements (800 maximum)
11-15 Number of different materials (12 max)
16-20 Number of boundary pressure cards (200 max)
21-30 Axial acceleration in the Z-direction
31-40 Angular velocity
41-50 Reference temperature (stress free temp.)
51-55 Number of approximations

If the number in column 10 is

0 XR is the specified R-load and
XZ is the specified Z-load
1 XR is the specified R-displacement and
XZ is the specified Z-load
2 XR is the specified R-load and
XZ is the specified Z-displacement
3 XR is the specified R-displacement and
XZ is the specified Z-displacement

All loads are considered to be total forces acting on a one radian segment.
Nodal point cards must be in numerical sequence. If cards are omitted, the omitted nodal points are generated at equal intervals along a straight line between the defined nodal points. The necessary temperatures are determined by linear interpolation. The boundary code (column 10), XR and XZ are set equal to zero.

E. ELEMENT CARDS - (6I5)
One card for each element

Columns		
1-5	Element number	1. Order nodal points clockwise around element.
6-10	Nodal Point I	
11-15	Nodal Point J	
16-20	Nodal Point K	2. Maximum difference between nodal point I. D. must be less than 27.
21-25	Nodal Point L	
26-30	Material Identification	

Element cards must be in element number sequence. If element cards are omitted, the program automatically generates the omitted information by incrementing by one the preceding I, J, K and L. The material identification code for the generated cards is set equal to the value given on the last card. The last element card must always be supplied.

Triangular elements are also permissible, and are identified by repeating the last nodal point number (i.e., I, J, K, K).

C. MATERIAL PROPERTY INFORMATION
The following group of cards must be supplied for each different material:

First card - (2I5, 2F10.0)

Columns	
1-5	Materials identification - any number from 1-12
6-10	Number of different temperatures for which properties are given - 8 maximum
11-20	Mass density of material
21-30	Ratio of plastic modulus to elastic modulus

Following cards - (8F10.0) One card for each temperature

Columns	
1-10	Temperature
11-20	Modulus of elasticity E_r and E_z
21-30	Poisson's ratio - ν_{rz}
31-40	Modulus of electricity - E_θ
41-50	Poisson's ratio $\nu_{\theta r}$ and $_{\theta z}$
51-60	Coefficient of thermal expansion - α_r and α_z
61-70	Coefficient of thermal expansion α_θ

71-80 Yield stress - σ_y

D. NODAL POINT CARDS - (2I5, 5F10.0)
One card for each nodal point with the following information:

Column	1-5	Nodal point number
	6-10	Number which indicates if displacements or forces are to be specified
	11-20	R - ordinate
	21-30	Z - ordinate
	31-40	XR
	41-50	XZ
	51-60	Temperature

F. PRESSURE CARDS (2I5, 1F10.0)
One card for each boundary element which is subjected to a normal pressure.

Column	1-5	Nodal Point I
	6-10	Nodal Point J
	11-20	Normal Pressure

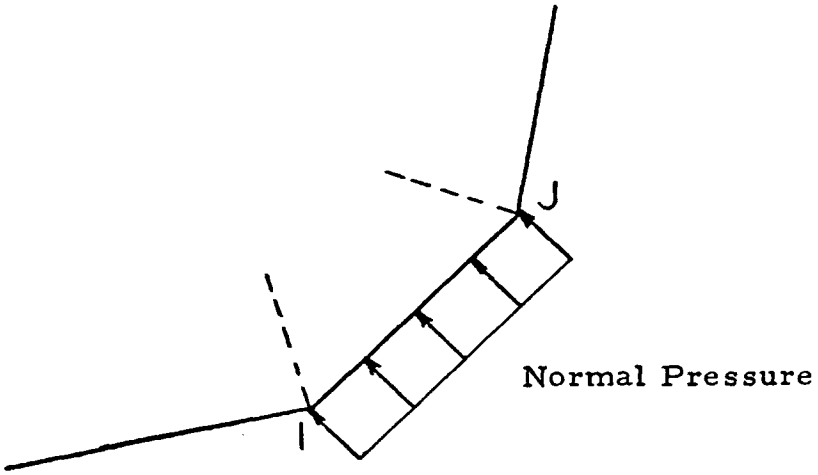

As shown above, the boundary element must be on the left as one progresses from I to J. Surface tensile force is input as a negative pressure.

ADDITIONAL REMARKS ON USE OF THE PROGRAM:
The previous section contains a schematic description of the program input. The purpose of this section is to explain in greater detail the various options of the program.

A. OUTPUT INFORMATION
The following information is developed and printed by the program:

1. Reprint of input data
2. Nodal point desplacements
3. Stresses at the center of each element
4. An approximate fundamental frequency. (The displacements for the given load condition are used as an approximate mode shape in the calculation of a frequency by Raleigh's procedure. A considerable amount of engineering judgment must be used in the intrpretation of this frequency.)

B. MATERIAL PROPERTIES

Material properties vs. temperature are input for each material in tabular form. The properties for each element in the system are then evaluated by interpolation. The mass density of the material is required only if acceleration loads are specified or if the approximate frequency is desired. Listing of the coefficients of thermal expansion are necessary only for thermal stress analysis. The plastic modulus ratio and the yield stress are specified only if nonlinear materials are used.

C. SKEW BOUNDARIES

If the number in columns 5-10 of the nodal point cards is other than 0, 1, 2, or3, it is interpreted as the magnitude of an angle in degrees. This angle is shown below.

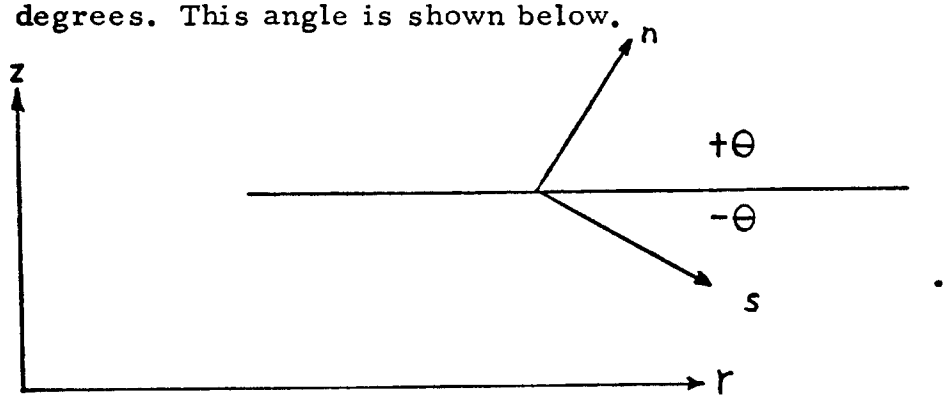

The terms in columns 31-50 of the nodal point card are then interpreted as follows:

XR is the specified load in the s-direction

XZ is the specified displacement in the n-direction

The angle θ must always be input as a negative angle and may range from -.001 to-180 degrees. Hence, + 1.0 degree is the same as -170.0 degrees. The displacements of these nodal points which are printed by the program are:

u_r the displacement in the s-direction

u_z the displacement in the n-direction

```
$IBFTC MAIN    DECK
C      ARBITRARY AXISYMMETRIC SOLIDS
C
       COMMON NUMNP,NUMEL,NUMMAT,NUMPC,ACELZ,ANGFQ, BAND,TEMP,MTYPE,...
      1 HED(12),E(8,8,12),RO(12),XXNN(12),R(900),Z(900),UR(900),UZ(900
      2 CODE(900),T(900),IBC(200),JBC(200),PR(200),ANGLE(4)
       COMMON /ARG/ RRR(5),ZZZ(5),S(10,10),P(10),TT(4),LM(4),DD(3,3),
      1 HH(6,10),RR(4),ZZ(4),C(4,4),H(6,10),D(6,6),F(6,10),TP(6),XI(
      2 ,EE(7),IX(800,5),EPS(800)
       COMMON /BANARG/ MBAND,NUMBLK,B(108),A(108,54)
      ~~COMMON /PLANE/ NPP~~ delete
C
C*****************************************************************
C      READ AND PRINT OF CONTROL INFORMATION AND MATERIAL PROPERTIES
C*****************************************************************
   50 READ  (5,1000) HED,NUMNP,NUMEL,NUMMAT,NUMPC,ACELZ,ANGFQ,  ,NP,N
      WRITE (6,2000) HED,NUMNP,NUMEL,NUMMAT,NUMPC,ACELZ,ANGFQ,  ,NP
C
      ~~IF (NPP) 54,56,54~~ delete   add  IF(NUMNP)501,501,56
   ~~54 WRITE (6,2008)~~
   56 DO 59 M=1,NUMMAT
      READ (5,1001) MTYPE,NUMTC,RO(MTYPE),XXNN(MTYPE)
      WRITE (6,2011) MTYPE,NUMTC,RO(MTYPE),XXNN(MTYPE)
      READ (5,1005) ((E(I,J,MTYPE),J=1,8),I=1,NUMTC)
      WRITE (6,2010) ((E(I,J,MTYPE),J=1,8),I=1,NUMTC)
      DO 58 I=  NUMTC,8
      DO 58 J=1,8
   58 E(I,J,MTYPE)=E(NUMTC,J,MTYPE)
   59 CONTINUE
C
C*****************************************************************
C      READ AND PRINT OF NODAL POINT DATA
C*****************************************************************
      WRITE (6,2004)
      L=0
   60 READ  (5,1002) N,CODE(N),R(N),Z(N),UR(N),UZ(N),T(N)
      NL=L+1
      ZX=N-L
      DR=(R(N)-R(L))/ZX
      DZ=(Z(N)-Z(L))/ZX
      DT=(T(N)-T(L))/ZX
   70 L=L+1
      IF(N-L) 100,90,80
   80 CODE(L)=0.0
      R(L)=R(L-1)+DR
      Z(L)=Z(L-1)+DZ
      UR(L)=0.0
      UZ(L)=0.0
      T(L)=T(L-1)+DT
      GO TO 70
   90 WRITE (6,2002) (K,CODE(K),R(K),Z(K),UR(K),UZ(K),T(K),K=NL,N)
      IF(NUMNP-N) 100,110,60
  100 WRITE (6,2009) N
```

```
      CALL EXIT
  110 CONTINUE
C*************************************************************
C        READ AND PRINT OF ELEMENT PROPERTIES
C*************************************************************
      WRITE (6,2001)
      N=0
  130 READ (5,1003) M,(IX(M,I),I=1,5)
  140 N=N+1
      IF (M-N) 170,170,150
  150 IX(N,1)=IX(N-1,1)+1
      IX(N,2)=IX(N-1,2)+1
      IX(N,3)=IX(N-1,3)+1
      IX(N,4)=IX(N-1,4)+1
      IX(N,5)=IX(N-1,5)
  170 WRITE (6,2003) N,(IX(N,I),I=1,5)
      IF (M-N) 180,180,140
  180 IF (NUMEL-N) 190,190,130
  190 CONTINUE
C*************************************************************
C      READ AND PRINT OF PRESSURE BOUNDARY CONDITIONS
C*************************************************************
      IF (NUMPC) 290,310,290
  290 WRITE (6,2005)
      DO 300 L=1,NUMPC
      READ  (5,1004) IBC(L),JBC(L),PR(L)
  300 WRITE (6,2007) IBC(L),JBC(L),PR(L)
  310 CONTINUE
C*************************************************************
C      DETERMINE BAND WIDTH
C*************************************************************
      J=0
      DO 340 N=1,NUMEL
      DO 340 I=1,4
      DO 325 L=1,4
      KK=IABS(IX(N,I)-IX(N,L))
      IF (KK-J) 325,325,320
  320 J=KK
  325 CONTINUE
  340 CONTINUE
      MBAND=2*J+2
C*************************************************************
C      SOLVE NON-LINEAR STRUCTURE BY SUCCESSIVE APPROXIMATIONS
C*************************************************************
      DO 350 N=1,NUMEL
  350 EPS(N)=0.0
C
      DO 500 NNN=1,NP
C
C     FORM STIFFNESS MATRIX
C
      CALL STIFF
C
C     SOLVE FOR DISPLACEMENTS
C
```

```
      CALL BANSOL
C
      WRITE (6,2006) (N,B(2*N-1),B(2*N),N=1,NUMNP)
C
C     COMPUTE STRESSES
C
      CALL STRESS
C
  500 CONTINUE
C*****************************************************************
      GO TO 50
C*****************************************************************
 1000 FORMAT (12A6/4I5,3F10.2,2I5)
 1001 FORMAT (2I5,2F10.0)
 1002 FORMAT (I5,F5.0,5F10.0)
 1003 FORMAT (6I5)
 1004 FORMAT (2I5,F10.0)
 1005 FORMAT (8F10.0)
 2000 FORMAT (1H1 12A6/
     1 30HO NUMBER OF NODAL POINTS------ I3 /
     2 30HO NUMBER OF ELEMENTS---------- I3 /
     3 30HO NUMBER OF DIFF. MATERIALS--- I3 /
     4 30HO NUMBER OF PRESSURE CARDS---- I3 /
     5 30HO AXIAL ACCELERATION---------- E12.4/
     6 30HO ANGULAR VELOCITY------------ E12.4/
     7 30HO REFERENCE TEMPERATURE------- E12.4/
     8 30HO NUMBER OF APPROXIMATIONS---- I3)
 2001 FORMAT (49H1ELEMENT NO.       I     J     K     L     MATERIAL
 2002 FORMAT (I12,F12.2,2F12.3,2E24.7,F12.3)
 2003 FORMAT (1I13,4I6,1I12)
 2004 FORMAT (108H1NODAL POINT         TYPE  R-ORDINATE  Z-ORDINATE
    .1AD OR DISPLACEMENT  Z LOAD OR DISPLACEMENT TEMPERATURE )
 2005 FORMAT (29HOPRESSURE BOUNDARY CONDITIONS/ 24H     I     J     PR
     1URE )
 2006 FORMAT (12H1N.P. NUMBER 18X 2HUR 18X 2HUZ / (1I12,2F20.7))
 2007 FORMAT (2I6,F12.3)
~~2008 FORMAT (23HOPLANE STRESS STRUCTURE )~~ delete
 2009 FORMAT (26HONODAL POINT CARD ERROR N= I5)
 2010 FORMAT (15HO  TEMPERATURE 10X 5HE(RZ) 9X 6HNU(RZ) 11X 4HE(T)
     1 10X 5HNU(T) 6X 9HALPHA(RZ) 7X 8HALPHA(T) 15H   YIELD STRESS /
     2 (F15.2,7E15.5))
 2011 FORMAT (17HOMATERIAL NUMBER= I3, 30H, NUMBER OF TEMPERATURE C.
     1 I3, 15H, MASS DENSITY= E12.4 ,16H,MODULUS RATIO= E12.4 )
C 501 CONTINUE
      END
```

add

```
$IBFTC STIF    DECK
      SUBROUTINE STIFF
C
      COMMON NUMNP,NUMEL,NUMMAT,NUMPC,ACELZ,ANGFQ, BAND,TEMP,MTYPE,Q,
     1 HED(12),E(8,8,12),RO(12),XXNN(12),R(900),Z(900),UR(900),UZ(90
     2 CODE(900),T(900),IBC(200),JBC(200),PR(200),ANGLE(4)
      COMMON /ARG/ RRR(5),ZZZ(5),S(10,10),P(10),TT(4),LM(4),DD(3,3),
     1 HH(6,10),RR(4),ZZ(4),C(4,4),H(6,10),D(6,6),F(6,10),TP(6),XI(1
     2 ,EE(7),IX(800,5),EPS(800)
      COMMON /BANARG/ MBAND,NUMBLK,B(108),A(108,54)
      COMMON /PLANE/ NPP
C                    delete
C*****************************************************************
C     INITIALIZATION
C*****************************************************************
      REWIND 2
      NB=27
      ND=2*NB
      ND2=2*ND
      STOP=0.0
      NUMBLK=0
C
      DO 50 N=1,ND2
      B(N)=0.0
      DO 50 M=1,ND
   50 A(N,M)=0.0
C*****************************************************************
C     FORM STIFFNESS MATRIX IN BLOCKS
C*****************************************************************
   60 NUMBLK=NUMBLK+1
      NN=NB*(NUMBLK+1)
      NM=NN-NB
      NL=NM-NB+1
      KSHIFT=2*NL-2
C
      DO 210 N=1,NUMEL
C
      IF (IX(N,5)) 210,210,65
   65 DO 80 I=1,4
      IF (IX(N,I)-NL) 80,70,70
   70 IF (IX(N,I)-NM) 90,90,80
   80 CONTINUE
      GO TO 210
C
   90 CALL QUAD(N,VOL)
C
      IF(VOL) 142,142,144
  142 WRITE (6,2003) N
      STOP=1.0
  144 IF(IX(N,3)-IX(N,4)) 145,165,145
  145 DO 150 II=1,9
      CC=S(II,10)/S(10,10)
      P(II)=P(II)-CC*P(10)
      DO 150 JJ=1,9
```

```
  150 S(II,JJ)=S(II,JJ)-CC*S(10,JJ)
C
      DO 160 II=1,8
      CC=S(II,9)/S(9,9)
      P(II)=P(II)-CC*P(9)
      DO 160 JJ=1,8
  160 S(II,JJ)=S(II,JJ)-CC*S(9,JJ)
C
C           ADD ELEMENT STIFFNESS TO TOTAL STIFFNESS
C
  165 DO 166 I=1,4
  166 LM(I)=2*IX(N,I)-2
C
      DO 200 I=1,4
      DO 200 K=1,2
      II=LM(I)+K-KSHIFT
      KK=2*I-2+K
      B(II)=B(II)+P(KK)
      DO 200 J=1,4
      DO 200 L=1,2
      JJ=LM(J)+L-II+1-KSHIFT
      LL=2*J-2+L
      IF(JJ) 200,200,175
  175 IF(ND-JJ) 180,195,195
  180 WRITE (6,2004) N
      STOP=1.0
      GO TO 210
  195 A(II,JJ)=A(II,JJ)+S(KK,LL)
  200 CONTINUE
  210 CONTINUE
C
C     ADD CONCENTRATED FORCES WITHIN BLOCK
C
      DO 250 N=NL,NM
      K=2*N-KSHIFT
      B(K)=B(K)+UZ(N)
  250 B(K-1)=B(K-1)+UR(N)
C
C     BOUNDARY CONDITIONS
C
C       1. PRESSURE B.C.
C
      IF (NUMPC) 260,310,260
  260 DO 300 L=1,NUMPC
      I=IBC(L)
      J=JBC(L)
      PP=PR(L)/6.
      DZ=(Z(I)-Z(J))*PP
      DR=(R(J)-R(I))*PP
      RX=2.0*R(I)+R(J)
      ZX=R(I)+2.0*R(J)
      IF (NPP) 262,264,262
  262 RX=3.0
      ZX=3.0
  264 II=2*I-KSHIFT
```

delete

```
      JJ=2*J-KSHIFT
      IF (II) 280,280,265
  265 IF (II-ND) 270,270,280
  270 SINA=0.0
      COSA=1.0
      IF (CODE(I)) 271,272,272
  271 SINA=SIN(CODE(I))
      COSA=COS(CODE(I))
  272 B(II-1)=B(II-1)+RX*(COSA*DZ+SINA*DR)
      B(II)=B(II)-RX*(SINA*DZ-COSA*DR)
  280 IF (JJ) 300,300,285
  285 IF (JJ-ND) 290,290,300
  290 SINA=0.0
      COSA=1.0
      IF (CODE(J)) 291,292,292
  291 SINA=SIN(CODE(J))
      COSA=COS(CODE(J))
  292 B(JJ-1)=B(JJ-1)+ZX*(COSA*DZ+SINA*DR)
      B(JJ)=B(JJ)-ZX*(SINA*DZ-COSA*DR)
  300 CONTINUE
C
C       2. DISPLACEMENT B.C.
C
  310 DO 400 M=NL,NH
      IF (M-NUMNP) 315,315,400
  315 U=UR(M)
      N=2*M-1-KSHIFT
      IF (CODE(M)) 390,400,316
  316 IF (CODE(M)-1.) 317,370,317
  317 IF (CODE(M)-2.) 318,390,318
  318 IF (CODE(M)-3.) 390,380,390
  370 CALL MODIFY(A,B,ND2,MBAND,N,U)
      GO TO 400
  380 CALL MODIFY(A,B,ND2,MBAND,N,U)
  390 U=UZ(M)
      N=N+1
      CALL MODIFY(A,B,ND2,MBAND,N,U)
  400 CONTINUE
C
C     WRITE BLOCK OF EQUATIONS ON TAPE AND SHIFT UP LOWER BLOCK
C
      WRITE (2) (B(N),(A(N,M),M=1,MBAND),N=1,ND)
C
      DO 420 N=1,ND
      K=N+ND
      B(N)=B(K)
      B(K)=0.0
      DO 420 M=1,ND
      A(N,M)=A(K,M)
  420 A(K,M)=0.0
C
C     CHECK FOR LAST BLOCK
C
      IF (NM-NUMNP) 60,480,480
  480 CONTINUE
```

```
C*************************************************************
      IF(STOP) 490,500,490
  490 CALL EXIT
  500 RETURN
C
 2003 FORMAT (26H0NEGATIVE AREA ELEMENT NO. I4)
 2004 FORMAT (29H0BAND WIDTH EXCEEDS ALLOWABLE I4)
      END
```

```
$IBFTC QUDF    DECK
      SUBROUTINE QUAD(N,VOL)
C
      COMMON NUMNP,NUMEL,NUMMAT,NUMPC,ACELZ,ANGFQ,MBAND,TEMP,MTYPE,
     1 HED(12),E(8,8,12),RO(12),XXNN(12),R(900),Z(900),UR(900),UZ(9
     2 CODE(900),T(900),IBC(200),JBC(200),PR(200),ANGLE(4)
      COMMON /ARG/ RRR(5),ZZZ(5),S(10,10),P(10),TT(4),LM(4),DD(3,3
     1 HH(6,10),RR(4),ZZ(4),C(4,4),H(6,10),D(6,6),F(6,10),TP(6),XI
     2 ,EE(7),IX(800,5),EPS(800)
      COMMON /BANARG/ ND,NUMBLK,B(108),A(108,54)
      COMMON /PLANE/ NPP
C
   90 I=IX(N,1)
      J=IX(N,2)
      K=IX(N,3)
      L=IX(N,4)
      MTYPE=IX(N,5)
      IX(N,5)=-IX(N,5)
C
C           FORM STRESS-STRAIN RELATIONSHIP
C
      TEMP=(T(I)+T(J)+T(K)+T(L))/4.0
      DO 103 M=2,8
      IF (E(M,1,MTYPE)-TEMP) 103,104,104
  103 CONTINUE
  104 RATIO=0.0
      DEN=E(M,1,MTYPE)-E(M-1,1,MTYPE)
      IF (DEN) 70,71,70
   70 RATIO=(TEMP-E(M-1,1,MTYPE))/DEN
   71 DO 105 KK=1,7
  105 EE(KK)=E(M-1,KK+1,MTYPE)+RATIO*(E(M,KK+1,MTYPE)-E(M-1,KK+1,MT
      TEMP=TEMP-Q
C
C
      EPSR=EE(7)/EE(1)
      IF (EPSR-EPS(N)) 106,108,108
  106 RATIO=(EE(7)/(EPS(N)*EE(1)))*(1.0-XXNN(MTYPE))+XXNN(MTYPE)
      EE(1)=EE(1)*RATIO
      EE(3)=EE(3)*RATIO
  108 CONTINUE
C
      IF (NPP) 84,86,84
   84 XX=EE(1)/EE(3)
      COMM=EE(1)/(XX-EE(2)**2)
      C(1,1)=COMM*XX
      C(1,2)=COMM*EE(2)
      C(1,3)=0.0
      C(2,1)=C(1,2)
      C(2,2)=COMM
      C(2,3)=0.0
      C(3,1)=0.0
      C(3,2)=0.0
      C(3,3)=0.0
      C(4,4)=.5*EE(1)/(XX+EE(2))
```

delete

delete

```
      ~~+3 TO 88~~
C
   86 C(1,1)=1.0/EE(1)
      C(1,2)=-EE(2)/EE(1)
      C(1,3)=-EE(4)/EE(3)
      C(2,1)=C(1,2)
      C(2,2)=C(1,1)
      C(2,3)=C(1,3)
      C(3,1)=C(1,3)
      C(3,2)=C(2,3)
      C(3,3)=1.0/EE(3)
      CALL SYMINV(C,3)
      C(4,4)=EE(1)/(2.0+2.0*EE(2))
C
   88 DO 110 M=1,3
  110 TT(M)=((C(M,1)+C(M,2))*EE(5)+C(M,3)*EE(6))*TEMP
C
C           FORM QUADRILATERAL STIFFNESS MATRIX
C
      RRR(5)=(R(I)+R(J)+R(K)+R(L))/4.0
      ZZZ(5)=(Z(I)+Z(J)+Z(K)+Z(L))/4.0
      DO 94 M=1,4
      MM=IX(N,M)
      IF(NPP) 93,89,93
   89 IF (R(MM)) 93,91,93
   91 R(MM)=.01*RRR(5)
      IF (CODE(MM)) 93,92,93
   92 CODE(MM)=1.0
   93 RRR(M)=R(MM)
   94 ZZZ(M)=Z(MM)
C
      DO 100 II=1,10
      P(II)=0.0
      DO 95 JJ=1,6
   95 HH(JJ,II)=0.0
      DO 100 JJ=1,10
  100 S(II,JJ)=0.0
      DO 119 II=1,4
      JJ=IX(N,II)
  119 ANGLE(II)=CODE(JJ)/57.3
C
      IF (K-L) 125,120,125
  120 CALL TRISTF(1,2,3)
      RRR(5)=(RRR(1)+RRR(2)+RRR(3))/3.0
      ZZZ(5)=(ZZZ(1)+ZZZ(2)+ZZZ(3))/3.0
      VOL=XI(1)
      GO TO 130
  125 VOL=0.0
      CALL TRISTF(4,1,5)
      VOL=VOL+XI(1)
      CALL TRISTF(1,2,5)
      VOL=VOL+XI(1)
      CALL TRISTF(2,3,5)
      VOL=VOL+XI(1)
      CALL TRISTF(3,4,5)
```

```
      VOL=VOL+XI(1)
C
      DO 140 II=1,6
      DO 140 JJ=1,10
  140 HH(II,JJ)=HH(II,JJ)/4.0
C
  130 RETURN
C
      END
```

```
$IBFTC TRIST   DECK
      SUBROUTINE TRISTF(II,JJ,KK)
C
      COMMON NUMNP,NUMEL,NUMMAT,NUMPC,ACELZ,ANGFQ,MBAND,TEMP,MTYPE,
     1 HED(12),E(8,8,12),RO(12),XXNN(12),R(900),Z(900),UR(900),UZ(9
     2 CODE(900),T(900),IBC(200),JBC(200),PR(200),ANGLE(4)
      COMMON /ARG/ RRR(5),ZZZ(5),S(10,10),P(10),TT(4),LM(4),DD(3,3),
     1 HH(6,10),RR(4),ZZ(4),C(4,4),H(6,10),D(6,6),F(6,10),TP(6),XI(
     2 ,EE(7),IX(800,5),EPS(800)
      COMMON /PLANE/ NPP
C
C        1. INITIALIZATION
C
      LM(1)=II
      LM(2)=JJ
      LM(3)=KK
C
      RR(1)=RRR(II)
      RR(2)=RRR(JJ)
      RR(3)=RRR(KK)
      RR(4)=RRR(II)
      ZZ(1)=ZZZ(II)
      ZZ(2)=ZZZ(JJ)
      ZZ(3)=ZZZ(KK)
      ZZ(4)=ZZZ(II)
C
   85 DO 100 I=1,6
      DO 90 J=1,10
      F(I,J)=0.0
   90 H(I,J)=0.0
      DO 100 J=1,6
  100 D(I,J)=0.0
C
C        3. FORM INTEGRAL(G)T*(C)*(G)
C
      CALL INTER(XI,RR,ZZ)
C
      D(2,6)=XI(1)*(C(1,2)+C(2,3))
      D(3,5)=XI(1)*C(4,4)
      D(5,5)=XI(1)*C(4,4)
      D(6,6)=XI(1)*C(2,2)
      IF (NPP) 104,106,104
  104 D(2,2)=XI(1)*C(1,1)
      D(3,3)=XI(1)*C(4,4)
      GO TO 108
  106 D(1,1)=XI(3)*C(3,3)
      D(1,2)=XI(2)*(C(1,3)+C(3,3))
      D(1,3)=XI(5)*C(3,3)
      D(1,6)=XI(2)*C(2,3)
      D(2,2)=XI(1)*(C(1,1)+2.0*C(1,3)+C(3,3))
      D(2,3)=XI(4)*(C(1,3)+C(3,3))
      D(3,3)=XI(6)*C(3,3)+XI(1)*C(4,4)
      D(3,6)=XI(4)*C(2,3)
C
  108 DO 110 I=1,6
```

delete

```
      DO 110 J=I,6
  110 D(J,I)=D(I,J)
C
C       4. FORM  COEFFICIENT-DISPLACEMENT TRANSFORMATION MATRIX
C
      COMM=RR(2)*(ZZ(3)-ZZ(1))+RR(1)*(ZZ(2)-ZZ(3))+RR(3)*(ZZ(1)-ZZ(2
      DD(1,1)=(RR(2)*ZZ(3)-RR(3)*ZZ(2))/COMM
      DD(1,2)=(RR(3)*ZZ(1)-RR(1)*ZZ(3))/COMM
      DD(1,3)=(RR(1)*ZZ(2)-RR(2)*ZZ(1))/COMM
      DD(2,1)=(ZZ(2)-ZZ(3))/COMM
      DD(2,2)=(ZZ(3)-ZZ(1))/COMM
      DD(2,3)=(ZZ(1)-ZZ(2))/COMM
      DD(3,1)=(RR(3)-RR(2))/COMM
      DD(3,2)=(RR(1)-RR(3))/COMM
      DD(3,3)=(RR(2)-RR(1))/COMM
C
      DO 120 I=1,3
      J=2*LM(I)-1
      H(1,J)=DD(1,I)
      H(2,J)=DD(2,I)
      H(3,J)=DD(3,I)
      H(4,J+1)=DD(1,I)
      H(5,J+1)=DD(2,I)
  120 H(6,J+1)=DD(3,I)
C
C     ROTATE UNKNOWNS IF REQUIRED
C
      DO 125 J=1,2
      I=LM(J)
      IF (ANGLE(I)) 122,125,125
  122 SINA=SIN(ANGLE(I))
      COSA=COS(ANGLE(I))
      IJ=2*I
      DO 124 K=1,6
      TEM=H(K,IJ-1)
      H(K,IJ-1)=TEM*COSA+H(K,IJ)*SINA
  124 H(K,IJ)= -TEM*SINA+H(K,IJ)*COSA
  125 CONTINUE
C
C       5. FORM ELEMENT STIFFNESS MATRIX (H)T*(D)*(H)
C
      DO 130 J=1,10
      DO 130 K=1,6
      IF (H(K,J)) 128,130,128
  128 DO 129 I=1,6
  129 F(I,J)=F(I,J)+D(I,K)*H(K,J)
  130 CONTINUE
C
      DO 140 I=1,10
      DO 140 K=1,6
      IF (H(K,I)) 138,140,138
  138 DO 139 J=1,10
  139 S(I,J)=S(I,J)+H(K,I)*F(K,J)
  140 CONTINUE
C
```

```
C      6. FORM THERMAL LOAD MATRIX
C
      IF (NPP) 145,150,145
  145 TT(3)=0.0
      COMM=XI(1)*EE(4)
  150 COMM=RO(MTYPE)*ANGFQ**2
      TP(1)=COMM*XI(7) + XI(2)*TT(3)
      TP(2)=COMM*XI(9) + XI(1)*(TT(1)+TT(3))
      TP(3)=COMM*XI(10)+ XI(4)*TT(3)
      COMM=-RO(MTYPE)*ACELZ
      TP(4)=COMM*XI(1)
      TP(5)=COMM*XI(7)
      TP(6)=COMM*XI(8) +XI(1)*TT(2)
C
      DO 160 I=1,10
      DO 160 K=1,6
  160 P(I)=P(I)+H(K,I)*TP(K)
C
C
C     FORM STRAIN TRANSFORMATION MATRIX
C
  400 DO 410 I=1,6
      DO 410 J=1,10
  410 HH(I,J)=HH(I,J)+H(I,J)
C
      RETURN
C
      END
```

delete

```
$IBFTC STRES   DECK
      SUBROUTINE STRESS
C
      COMMON NUMNP,NUMEL,NUMMAT,NUMPC,ACEL7,ANGFQ,MBAND,IEMP,MTYPE,
     1 HED(12),E(8,8,12),RO(12),XXNN(12),R(900),Z(900),UR(900),UZ(9
     2 CODE(900),T(900),IBC(200),JBC(200),PR(200),ANGLE(4),SIG(10)
      COMMON /ARG/ RRR(5),ZZZ(5),S(10,10),P(10),TT(4),LM(4),DD(3,3),
     1 HH(6,10),RR(4),ZZ(4),C(4,4),H(6,10),D(6,6),F(6,10),TP(6),XI(
     2 ,EE(7),IX(800,5),EPS(800)
      COMMON /BANARG/ ND,NUMBLK,B(108),A(108,54)
      ~~COMMON /PLANE/ NPP~~ delete
C*****************************************************************
C     COMPUTE ELEMENT STRESSES
C*****************************************************************
      XKE=0.0
      XPE=0.0
      MPRINT=0
C
      DO 300 M=1,NUMEL
C
      N=M
      IX(N,5)=IABS(IX(N,5))
      MTYPE=IX(N,5)
C
      CALL QUAD(N,VOL)
      IX(N,5)=MTYPE
C
      DO 120 I=1,4
      II=2*I
      JJ=2*IX(N,I)
      P(II-1)=B(JJ-1)
  120 P(II)=B(JJ)
C
      DO 150 I=1,2
      RR(I)=P(I+8)
      DO 150 K=1,8
  150 RR(I)=RR(I)-S(I+8,K)*P(K)
C
      COMM=S(9,9)*S(10,10)-S(9,10)*S(10,9)
      IF (COMM) 155,160,155
  155 P(9)=(S(10,10)*RR(1)-S(9,10)*RR(2))/COMM
      P(10)=(-S(10,9)*RR(1)+S(9,9)*RR(2))/COMM
C
  160 DO 170 I=1,6
      TP(I)=0.0
      DO 170 K=1,10
  170 TP(I)=TP(I)+HH(I,K)*P(K)
C
C
      RR(1)=TP(2)
      RR(2)=TP(6)
      RR(3)=(TP(1)+TP(2)*RRR(5)+TP(3)*ZZZ(5))/RRR(5)
      RR(4)=TP(3)+TP(5)
C
```

```
  176 DO 180 I=1,3
      SIG(I)=-TT(I)
      DO 180 K=1,3
  180 SIG(I)=SIG(I)+C(I,K)*RR(K)
      SIG(4)=C(4,4)*RR(4)
C
C     CALCULATE ENERGY TERMS
C
      DO 250 I=1,10
      COMM=0.0
      DO 200 K=1,10
  200 COMM=COMM+S(I,K)*P(K)
  250 XPE=XPE+COMM*P(I)
      XKE=XKE+VOL*RO(MTYPE)*(P(9)**2+P(10)**2)
C
C     CALCULATE EFFECTIVE STRAIN
C
      IF (NPP) 251,252,251
  251 RR(3)=-(SIG(1)+SIG(2))*EE(2)/EE(1)
  252 CC=(RR(1)+RR(2))/2.0
      CR=SQRT( ((RR(2)-RR(1))/2.0)**2 + (RR(4)/2.0)**2 )
      RR(1)=CC+CR
      RR(2)=CC-CR
      EPS(N)=SQRT((RR(1)-RR(2))**2+(RR(1)-RR(3))**2+(RR(2)-RR(3))**2)
     1 *.707/(1.0+EE(2))
C
C*************************************************************************
      OUTPUT STRESSES
C*************************************************************************
C
C     CALCULATE PRINCIPAL STRESSES
C
      CC=(SIG(1)+SIG(2))/2.0
      BB=(SIG(1)-SIG(2))/2.
      CR=SQRT(BB**2+SIG(4)**2)
      SIG(5)=CC+CR
      SIG(6)=CC-CR
      SIG(7)=28.648*ATAN2(SIG(4),BB)
C
C     STRESSES PARALLEL TO LINE I-J
C
      I=IX(N,1)
      J=IX(N,2)
      ANG=2.*ATAN2(Z(J)-Z(I),R(J)-R(I))
      COS2A=COS(ANG)
      SIN2A=SIN(ANG)
      CX=.5*(SIG(1)-SIG(2))
      SIG(8)=CX*COS2A+SIG(4)*SIN2A+CC
      SIG(9)=2.*CC-SIG(8)
      SIG(10)=-CX*SIN2A+SIG(4)*COS2A
C
  104 IF (MPRINT) 110,105,110
  105 WRITE (6,2000)
      MPRINT=50
  110 MPRINT=MPRINT-1
```

```
C
  305 WRITE (6,2001)  N,RRR(5),ZZZ(5),(SIG(I),I=1,10)
  300 CONTINUE
C
      IF (XKE) 310,320,310
  310 W=SQRT(XPE/XKE)
      WRITE (6,2006) W
C
  320 RETURN
C
 2000 FORMAT (7H1EL.NO.  7X 1HR  7X 1HZ 4X 8HR-STRESS 4X 8HZ-STRESS 4
     1 8HT-STRESS 3X 9HRZ-STRESS 2X 10HMAX-STRESS 2X 10HMIN-STRESS
     2 37H  ANGLE IJ-STRESS JK-STRESS     SHEAR )
 2001 FORMAT (I7,2F8.2,1P6E12.4,0P1F7.2,1P3E10.2)
 2006 FORMAT (36HOAPPROXIMATE FUNDAMENTAL FREQUENCY = E12.5)
C
      END
```

```
$IBFTC SYMI    DECK
      SUBROUTINE SYMINV(A,NMAX)
C
      DIMENSION A(4,4)
C
      DO 200 N=1,NMAX
C
      D=A(N,N)
      DO 100 J=1,NMAX
  100 A(N,J)=-A(N,J)/D
C
      DO 150 I=1,NMAX
      IF(N-I) 110,150,110
  110 DO 140 J=1,NMAX
      IF(N-J) 120,140,120
  120 A(I,J)=A(I,J)+A(I,N)*A(N,J)
  140 CONTINUE
  150 A(I,N)=A(I,N)/D
C
      A(N,N)=1.0/D
C
  200 CONTINUE
C
      RETURN
C
      END
```

```
$IBFTC INTE    DECK
      SUBROUTINE INTER(XI,RR,ZZ)
C
      DIMENSION RR(1),ZZ(1),XI(1),XM(6),R(6),Z(6),XX(6)
      COMMON /PLANE/ NPP
      DATA (XX(I),I=1,6)/3*1.0,3*3.0/
C
      COMM=RR(2)*(ZZ(3)-ZZ(1))+RR(1)*(ZZ(2)-ZZ(3))+RR(3)*(ZZ(1)-ZZ(2
      COMM=COMM/24.0
      R(1)=RR(1)
      R(2)=RR(2)
      R(3)=RR(3)
      R(4)=(R(1)+R(2))/2.
      R(5)=(R(2)+R(3))/2.
      R(6)=(R(3)+R(1))/2.
C
      Z(1)=ZZ(1)
      Z(2)=ZZ(2)
      Z(3)=ZZ(3)
      Z(4)=(Z(1)+Z(2))/2.
      Z(5)=(Z(2)+Z(3))/2.
      Z(6)=(Z(3)+Z(1))/2.
C
      IF (NPP) 10,30,10
   10 DO 20 I=1,6
   20 XM(I)=XX(I)
      GO TO 40
   30 DO 35 I=1,6
   35 XM(I)=XX(I)*R(I)
C
   40 DO  50 I=1,10
   50 XI(I)=0.0
C
      DO 100 I=1,6
      XI(1)=XI(1)+XM(I)
      XI(2)=XI(2)+XM(I)/R(I)
      XI(3)=XI(3)+XM(I)/(R(I)**2)
      XI(4)=XI(4)+XM(I)*Z(I)/R(I)
      XI(5)=XI(5)+XM(I)*Z(I)/(R(I)**2)
      XI(6)=XI(6)+XM(I)*Z(I)**2/(R(I)**2)
      XI(7)=XI(7)+XM(I)*R(I)
      XI(8)=XI(8)+XM(I)*Z(I)
      XI(9)=XI(9)+XM(I)*R(I)**2
      XI(10)=XI(10)+XM(I)*R(I)*Z(I)
  100 CONTINUE
C
      DO 150 I=1,10
  150 XI(I)=XI(I)*COMM
C
      RETURN
C
      END
```

delete

```
$IBFTC MODI     DECK
       SUBROUTINE MODIFY(A,B,NEQ,MBAND,N,U)
C
       DIMENSION A(108,54),B(108)
C
       DO 250 M=2,MBAND
       K=N-M+1
       IF(K) 235,235,230
  230  B(K)=B(K)-A(K,M)*U
       A(K,M)=0.0
  235  K=N+M-1
       IF(NEQ-K) 250,240,240
  240  B(K)=B(K)-A(N,M)*U
       A(N,M)=0.0
  250  CONTINUE
       A(N,1)=1.0
       B(N)=U
       RETURN
C
       END
```

```
$IBFTC BANS    DECK
      SUBROUTINE BANSOL
C
      COMMON /BANARG/ MM,NUMBLK,B(108),A(108,54)
C
      NN=54
      NL=NN+1
      NH=NN+NN
      REWIND 1
      REWIND 2
      NB=0
      GO TO 150
C*****************************************************************
C     REDUCE EQUATIONS BY BLOCKS
C*****************************************************************
C
C     1. SHIFT BLOCK OF EQUATIONS
C
  100 NB=NB+1
      DO 125 N=1,NN
      NM=NN+N
      B(N)=B(NM)
      B(NM)=0.0
      DO 125 M=1,MM
      A(N,M)=A(NM,M)
  125 A(NM,M)=0.0
C
C     2. READ NEXT BLOCK OF EQUATIONS INTO CORE
C
      IF (NUMBLK-NB) 150,200,150
  150 READ (2) (B(N),(A(N,M),M=1,MM),N=NL,NH)
      IF (NB) 200,100,200
C
C     3. REDUCE BLOCK OF EQUATIONS
C
  200 DO 300 N=1,NN
      IF (A(N,1)) 225,300,225
  225 B(N)=B(N)/A(N,1)
      DO 275 L=2,MM
      IF (A(N,L)) 230,275,230
  230 C=A(N,L)/A(N,1)
      I=N+L-1
      J=0
      DO 250 K=L,MM
      J=J+1
  250 A(I,J)=A(I,J)-C*A(N,K)
      B(I)=B(I)-A(N,L)*B(N)
      A(N,L)=C
  275 CONTINUE
  300 CONTINUE
C
C     4. WRITE BLOCK OF REDUCED EQUATIONS ON TAPE 2
C
      IF (NUMBLK-NB) 375,400,375
  375 WRITE (1) (B(N),(A(N,M),M=2,MM),N=1,NN)
```

```
      GO TO 100
C*****************************************************************
C     BACK-SUBSTITUTION
C*****************************************************************
  400 DO 450 M=1,NN
      N=NN+1-M
      DO 425 K=2,MM
      L=N+K-1
  425 B(N)=B(N)-A(N,K)*B(L)
      NM=N+NN
      B(NM)=B(N)
  450 A(NM,NB)=B(N)
      NB=NB-1
      IF (NB) 475,500,475
  475 BACKSPACE 1
      READ (1) (B(N),(A(N,M),M=2,MM),N=1,NN)
      BACKSPACE 1
      GO TO 400
C*****************************************************************
C     ORDER UNKNOWNS IN B ARRAY
C*****************************************************************
  500 K=0
      DO 600 NB=1,NUMBLK
      DO 600 N=1,NN
      NM=N+NN
      K=K+1
  600 B(K)=A(NM,NB)
C
      RETURN
C
      END
```

BIBLIOGRAPHY

1. Leeman, E.R. "The Measurement of Stress in Rock: Parts I, II, III," Jounal of the South African Institute of Mining and Metallurgy, Sept.-Nov. 1964.

2. Galle, E.M. "Photoelastic Analysis of the Stresses Near the Bottom of a Cylindrical Cavity Due to Non-symmetrical Loading" M.S. Thesis, The Rice Institute, 1959.

3. Galle, E.M. and Wilhoit, J. "Stresses Around a Well Bore Due to Internal Pressure and Unequal Principal Geostatic Stresses" Society of Petroleum Engineers Journal, Vol. 2, 1962.

4. Hoskins, E. "An Investigation of Strain-Relief Methods of Measuring Rock Stress" International Journal of Rock Mechanics and Mining Sciences, Vol. 4, 1967.

5. Bonnechere, F. "A Comparative Study of InSitu Rock Stress Measurement Techniques" M.S. Thesis, University of Minnesota, 1967.

6. Bonnechere, F. and Fairhurst, C. "Determination of the Regional Stress Field from Doorstopper Measurements" Journal of the South African Institute of Mining and Metallurgy, July 1968.

7. Pallister, C.F. "The Effect of a Triaxial Stress Field at the Flat End of a Borehole Drilled Parallel to One of the Principal Stresses" Transvaal and Orange Free State Chamber of Mines Research Report No. 73/67, 1967.

8. Van Heerden, W. L. "Stress Concentration Factors for the Flat Borehole End for Use in Rock Stress Measurements" Engineering Geology, Vol. 3, 1969.

9. Hiramatsu, Y. and Oka, Y. "Determination of the Stress in Rock Unaffected by Boreholes or Drifts From Measured Strains or Deformations" International Journal of Rock Mechanics and Mining Sciences, July 1968.

10. Crouch, S. L. "A Note on the Stress Concentrations at the Bottom of a Flat Ended Borehole" Journal of the South African Institute of Mining and Metallurgy, December 1969.

11. Coates, D. F. and Yu, Y. S. "A Note on the Stress Concentrations at the End of a Cylindrical Hole" International Journal of Rock Mechanics and Mining Sciences, Vol. 7, 1970.

12. Terzaghi, K. and Richart, F. E. "Stress in Rock about Cavities" Geotechnique, Vol. 3, 1952.

13. Leeman, E. R. "Rock Stress Measurements Using the Trepanning Stress-Relieving Technique" Mine and Quarry Engineering, June 1964.

14. Van Heerden, W. L. and Grant, F. "A Comparison of Two Methods for Measuring Rock Stress in Rock" International Journal of Rock Mechanics and Mining Sciences, Vol. 4, No. 4, 1967.

15. Stephenson, B. R. and Murray, K. J. "Application of the Strain Rosette Relief Method to Measure Principal Stresses

Throughout a Mine" International Journal of Rock Mechanics and Mining Sciences, Vol 7, 1970.

16. Capozza, F., Martinetti, S. and Ribacchi, R. "Results of State- of-Stress Measurements in Rock Masses by Means of Borehole Devices" International Conference on Determination of Stresses, Lisbon, 1969.

17. Bonnechere, F. and Fairhurst, C. "Results of an In Situ Comparison of Different Techniques for Rock Stress Determination" International Conference of Determination of Stresses, Lisbon, 1969.

18. Coates, D.F. Private Communication, March 1972.

19. Obert, L. and Duvall, W. "Rock Mechanics and the Design of Structures in Rock" John Wiley and Sons Inc., New York.

20. Merrill, R.H. "Three- Component Borehole Deformation Gage for Determining the Stresses in Rock" USBM RI 7015.

21. Gray, W.M. and Barron, K. "Stress Determinations from Strain-Relief Measurements on the Ends of Boreholes; Planning, Data Evaluation and Error Assessment" International Conference of the Determination of Stresses, Lisbon, 1969.

22. Van Heerden, W.L. "Potential Fracture Zones Around Boreholes with Flat and Spherical Ends" International Journal of Rock Mechanics and Mining Sciences, Vol. 6, No. 5, 1969.

23. Leeman, E.R. "The Doorstopper and Triaxial Rock Stress

Measuring Instruments Developed by the C.S.I.R." Journal of the South African Institute of Mining and Metallurgy, February 1969.

24. Fairhurst, C. "Methods of Determining In Situ Rock Stresses at Great Depth" Technical Report 1-68, Missouri River Division, Corps of Engineers, February, 1968.

25. Leeman, E.R. "The Determination of the Complete State of Stress in Rock in a Single Borehole--Laboratory and Underground Measurements" International Journal of Rock Mechanics and Mining Sciences, Vol. 5, No. 1, 1968.